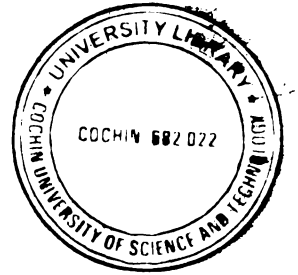


T405



**Studies on Chaos and Synchronization
in ac-driven Josephson junctions**

Thesis submitted to
Cochin University of Science and Technology
in partial fulfillment of the requirements
for the award of the degree of
Doctor of Philosophy


Chitra R Nayak
Department of Physics
Cochin University of Science and Technology
Kochi - 682022

October 2008

CERTIFICATE

Certified that the work presented in this thesis is a bonafide work done by Ms. Chitra R Nayak, under my guidance in the Department of Physics, Cochin University of Science and Technology and that this work has not been included in any other thesis submitted previously for the award of any degree.

Kochi
October 15, 2008


Dr. ~~V. C.~~ Kuriakose
(Supervising Guide)

DECLARATION

I hereby declare that the work presented in this thesis is based on the original work done by me under the guidance of Dr. V. C. Kuriakose, Professor (Rtd.), Department of Physics, Cochin University of Science and Technology and has not been included in any other thesis submitted previously for the award of any degree.

Kochi
October 15, 2008


Ms. Chitra R Nayak

Contents

Acknowledgements	v
Preface	ix
1 Josephson junctions	1
1.1 Josephson junction model	7
1.1.1 Short Josephson junctions	7
1.1.2 Long Josephson junctions	11
1.2 Chaos	17
1.2.1 Ways to characterize chaos	19
1.3 Different routes to chaos	24
1.3.1 Chaos in Josephson junctions	25
1.4 Synchronization of chaotic systems	27
1.4.1 Stability of synchronization	32
1.5 Outline of the thesis	33
2 Suppressing chaos in coupled Josephson junctions	35
2.1 Introduction	35
2.1.1 Coupled Josephson junctions	36

2.1.2	Lyapunov exponents	40
2.2	Synchronization of Josephson junctions	42
2.3	Controlling chaos	45
2.4	The effect of phase difference	47
2.5	Conclusion	55
3	Synchronization in an array of coupled Josephson junctions	59
3.1	Introduction	59
3.2	The model	60
3.3	Stability analysis	63
3.4	Phase effect	67
3.5	Result and discussion	70
4	Effect of phase difference on bidirectionally coupled system with time-delay	73
4.1	Time-delay systems	73
4.2	Time-delay equations	76
4.3	Stability analysis	77
4.4	Effect of phase difference and frequency detuning . . .	83
4.5	Result and discussion	86
5	Dynamics of semiannular Josephson junctions with external ac-biasing	89
5.1	Introduction	89
5.2	Semiannular Josephson junction	91
5.3	Perturbational analysis	95
5.3.1	Expression for potential function	97

5.3.2	Numerical methods	100
5.4	Creation and annihilation of fluxons	102
5.4.1	One fluxon solution	103
5.4.2	Two fluxon solution	104
5.4.3	Three fluxon solution	105
5.5	Chaos in semiannular Josephson junction	106
5.6	Conclusions	109
6	Results and discussion	111
A	Numerical Programs	115
A.1	Transverse Lyapunov Exponent	115
A.2	Finite Difference method for a semiannular Josephson Junction	122
	References	127

Acknowledgements

I am fortunate to work under the guidance of Dr. V. C. Kuriakose who has wide knowledge and a lot of research experience which helped me throughout the period of work. I would like to express my deep and sincere gratitude to him for patiently and affectionately correcting all my mistakes and guiding me with the right suggestions. His understanding, logical way of thinking and the way of tackling difficult situations in an easy manner has helped me immensely during the research work.

I wish to express my sincere thanks to Dr. Ramesh Babu T for being there as a constant source of support and providing help whenever I needed them most.

I take this opportunity to thank Dr. Godfrey Louis, Head of the Department of Physics and also the former Heads of the Department, Dr. K. P. Vijayakumar, Dr. V. C. Kuriakose and Dr. Ramesh Babu T for providing necessary facilities for my research work. I thank all the faculty members and office staff of this department, present and former, for all the support provided. The help and cooperation of the library staff is also gratefully acknowledged.

I thank Prof. M Lakshmanan, Centre for Nonlinear Dynamics, Bharathidasan University, Thiruchirapalli for the useful discussions and warm hospitality extended during my visit to the center. I also express my sincere gratitude to Prof. Neelima Gupte for helping at various stages of my research work. My sincere thanks to Dr. Ira B Schwartz, Naval Research Laboratory, Nonlinear Systems Dynamics Sections, USA for the valuable suggestions and help extended during the numerical works.

I thankfully remember the good times I had with the research scholars of this department and the various batches of M.Sc. and M.Phil. students who helped me to become a better person. Getting good friends is a luck and I think I am blessed with some good friends. I express my deep sense of gratitude to Dr. Minu Joy for her sisterly considerations and Dr. Ravikumar C D for the warm affection. I am thankful to Vinayaraj, Nijo, Vivek and Priyesh for the love and consideration they showered on me. Special thanks to Vinayaraj for the beautiful cover design of this thesis. I also thank Nima for her classic jokes, Dr. Subha P A for the kind advices and Bhavya and Lini for their friendship. I thank Reshmi, Asha, Deepa, Tina and Sreeja for the elite company they provided. Words are insufficient to express my gratitude to Jisha who is a wonderful friend and Sini who supported me during my ups and downs.

I take this opportunity to thank Dr. Santhi A whose friendship meant a lot to me and has been a constant source of motivation. Thanks to Dr. Rajesh, ISP, CUSAT who helped me during the initial stages of work. Without the help of Manu Punnen, ISP, the numerical works would have been difficult and I thank him for the

help and friendship offered.

I gratefully acknowledge the financial support provided by DRDO, Govt. of India, in the form of a research fellowship through a major research project and Cochin University of Science and Technology for providing me Junior Research Fellowship.

My special thanks to Peter chettan for the nice binding of this thesis. Days have been lovely due to the presence of Ananthu, Balu, Suma, Subha, Sreeni and ammoonma who filled the hours with happiness. I am extremely grateful to amma and appa who have been unbelievably supportive, without which it would have been impossible to lead such a long student life as I had. I am lucky to have Narayanamamu and Rohinimayi in my life, who supported my parents during a difficult time, without which I would not have been able to finish this thesis in time. I remember with warmth the care and support extended to me by Radhakrishnan as a good friend and partner.

I am thankful to God for making me who I am and giving me the courage to stand firm on my decisions.

Chitra R Nayak

Preface

Since the experimental observation of the Josephson effect, there has been continuously growing interest in the fundamental physics and the applications of this effect. The achievements in the Josephson junction technology has made it possible to develop a variety of sensors for detecting ultra low magnetic field, gravitational radiation and weak electromagnetic radiation and a number of devices. The study of coupled Josephson junctions has been stimulated by the interest in constructing coherent arrays of junctions for technical applications. Above all, Josephson junction has been proved to be an ideal candidate for studying nonlinear dynamics and chaos and hence the system is of fundamental theoretical interest. The study of the dynamics of Josephson junction is an area of great theoretical interest because of the richness of the dynamics of the junction. The supercurrent in Josephson junction has a highly nonlinear dependence on the applied electromagnetic field making it different from the nonlinear dynamics of other systems. The high sensitivity of the supercurrent to the electromagnetic field makes it highly sensitive to fluctuations in the applied fields and it makes the dynamics more

complex.

This thesis is devoted to the study of Josephson junction systems in the presence of an external ac biasing. The ac biasing when applied to a short Josephson junction represented by a second order differential equation becomes an ideal system to study chaos. The similarity of the equation of a short Josephson junction equation to the equation of a driven damped oscillator makes it a case where theoretical predictions can be experimentally verified, while the long Josephson junction is equivalent to the continuum limit of a chain of torsion coupled pendula immersed in a viscous medium and subject to an oscillatory torque. Hence these studies are very important experimentally as well as theoretically.

Chapter 1 gives a review on Josephson junctions, from its prediction to the equations describing various junction models necessary for the studies done in this thesis. The basic ideas of chaos and synchronization are also presented. A brief review on the works done in chaos in Josephson junctions is also presented and the importance of such studies is projected.

In **Chapter 2**, we discuss the case of two coupled Josephson junctions which are linked in parallel with a linking resistor R_s . The dynamics of the system is studied and the parameter space where the system exhibits chaotic motion is recognized. Lyapunov exponent spectrum reveals that the system is in chaotic regime for all values of coupling strength in the parameter regime considered. The effect of an applied phase difference on such a system is studied. The parameter regime in which the system is synchronized is identified and a small phase difference is found to desynchronize the system.

Large values of phase difference is found to suppress chaos and bring in periodic behavior. Lyapunov exponent spectrum in the presence of phase difference reveals that the system exhibits periodic behavior for certain range of values of coupling strength when the system is synchronized.

Chapter 3 is an extension of the work given in chapter 2 for an array of N Josephson junctions. For this, we start with a system of three Josephson junctions and study the synchronization behavior. It is found that the system exhibits the phenomenon of relay synchronization where two outer systems get synchronized while remaining uncorrelated with the middle system through which both are connected. This study is of relevance because of the similarity of the behavior of this model to the neural models currently studied. The stability of synchronization for the outer junctions is found and it is also shown that in the presence of an external drive the outer junctions do not synchronize with the middle one. Following this argument we show that for an array of N junctions, $N/2$ solutions can exist if the number of junctions is even and $(N + 1)/2$ solutions if the number of junctions is odd. In the presence of a phase difference between the external fields, the system exhibits periodic behavior with a definite phase relationship between all the three junctions.

In **Chapter 4** we consider an array of three Josephson junctions with a time-delay in the coupling term. Time-delayed systems find applications in secure communication and the bidirectional coupling makes two way transmission of signals possible. As in the previous case, in the chaotically synchronized manifold, we find that only the outer systems get synchronized while remaining uncorrelated with

the middle junction. The sum of the transverse Lyapunov exponents (TLE) are evaluated and is found to be negative. Comparing the cross-correlation and TLE spectrum, we show that we can get the qualitative nature of the spectrum in cases where the explicit calculation of TLE is not possible. The effect of time-delay on system dynamics and synchronization are also studied. The effect of phase difference between the applied fields and frequency detuning is also analyzed.

Semicircular Josephson junction was proved to be an ideal candidate to make Josephson junction based diode, rectifiers etc. In **Chapter 5** we study the influence of an applied ac biasing on a semicircular Josephson junction. We derive an expression for the potential in the presence of the external biasing following perturbational analysis. The effect of the oscillating potential on one fluxon, two fluxon and three fluxon input is studied. It is found the magnetic field along with the biasing induces creation and annihilation of fluxons in the junction. The I-V characteristics of the junction is studied by considering the surface loss term also in the model equation. The system is found to exhibit chaotic behavior in the presence of ac biasing.

In **Chapter 6** the results are briefed and the future works are presented. The fortran and matlab codes used for the numerical simulations are given in the Appendix.

Part of these investigations has been published/submitted in journals and presented in conferences.

List of papers published/presented/communicated:

International Journals

1. Dynamics of Coupled Josephson junction under the influence of applied fields **Chitra R Nayak** and V C Kuriakose, *Phys. Lett. A* **365**, 284 (2007)
2. Phase synchronization in an array of driven Josephson junctions , **Chitra R N** and V C Kuriakose, *Chaos* **18**, 013125 (2008), *Virtual Journal of Applications of Superconductivity* **14** Issue - 7, (2008).
3. Phase effects on synchronization by dynamical relaying in delay-coupled systems, **Chitra R N** and V C Kuriakose, *Chaos* **18**, 023129 (2008) *Virtual Journal of Applications of Superconductivity* **15** Issue - 1, (2008).
4. Creation and annihilation of fluxons in ac-driven semi-annular Josephson junction **Chitra R N** and V C Kuriakose, (Submitted to Super. Sci. Tech.).

Conferences

1. The effect of phase of the applied field on coupled Josephson junctions **Chitra R N** and V C Kuriakose, NCNSD, Madras University, 6-8 Febraury 2006.
2. Dynamics of a semicircular Josephson junction in the presence of an external magnetic field **Chitra R N**, Sonia Varghese and

V C Kuriakose, NHTEP 2007, Department of Physics, Cochin University of Science and Technology, 8-10 October 2007.

3. Synchronization in an array of three Josephson junctions
Chitra R N and V C Kuriakose, RDND 2008, Bharathidasan University, 13-16 February 2008 .

Chapter 1

Josephson junctions

Kammerlingh Onnes and his assistants in 1908 liquefied helium paving the way for experimenting at temperatures very close to absolute zero. In 1911, he observed that when the temperature was lowered to 4.3 K, the resistivity of mercury suddenly dropped to a near zero value. This phenomenon is now known as superconductivity. Later, it was understood that at a critical temperature T_c , the specimen would undergo a phase transition from a normal to a superconducting state. It was also observed that a superconductor is a perfect diamagnet in addition to being a perfect conductor. The superconducting state is an ordered state of the conduction electrons in the metal. The conduction electrons interact with the crystal lattice through phonons, and this effect gives rise to an effective attractive interaction between the electrons with opposite spin and angular momentum which then make the electrons to form a pair. Such pairs of electron with bosonic nature are called Cooper pairs.

All the Cooper pairs are in the Bose-condensed state at zero temperature and are separated by an energy gap Δ from the quasi particle state. The value of the energy gap is proportional to the effective binding energy of the Cooper pair. The energy gap depends on the temperature and as the temperature is increased, the value of the energy gap decreases and vanishes when the critical temperature is reached. Because of the bosonic nature, all the Cooper pairs can be represented by the ground state wave function,

$$\Psi = \sqrt{n} \exp(\theta), \quad (1.1)$$

where Ψ is often called the superconducting order parameter. n is the Cooper pair density while θ is the quantum mechanical phase factor. Later superconductivity phenomenon was discovered in many metals and alloys [1].

In 1962, B D Josephson predicted that several new interesting phenomena could be observed in the weak electrical contact between two superconductors [2]. When an insulator is present between two superconductors the value of the wave function reduces from its bulk value near the link. However the superconductors get weakly coupled to each other due to the small overlap between the macroscopic wave functions (Fig. 1.1). Josephson pointed that a supercurrent I_s will flow through the junction even in the absence of an external voltage, which is related to the voltage V developed across the junction by an unusual formula which follows directly from the basic ideas of quantum mechanics and contains the Planck's constant \hbar . Experimental evidence for the Josephson supercurrent was obtained in 1963

[3]. Josephson's discovery has not only contributed to the development of superconductivity, but also to the development of nonlinear dynamics as a whole. The Josephson junctions have enabled the engineers to develop several new devices with extraordinary characteristics which find immense applications in various fields of science and technology specially for producing huge magnetic fields [4, 5]. By the beginning of 1970's the study of Josephson junctions was divided into solid state physics and dynamics. In solid state physics, various expressions connecting $I(t)$ and $V(t)$ are derived from the theory of superconductivity. The aim of the dynamics part is to describe various phenomena observed using the relation between I and V . This latter part of the general theory has turned to be more difficult than the former one due to the more complex dynamical behavior shown by the system. The supercurrent has a highly nonlinear dependence on the electromagnetic field making it different from the nonlinear dynamics of other systems. The high sensitivity of the supercurrent to the electromagnetic field makes it highly sensitive to fluctuations and it makes the dynamics more complex [6]. When a voltage is applied, a current is produced in the junction and the study of the resulting current is interesting. Among the various dynamical behavior, chaotic dynamics has also been an active area of research. In this thesis, we concentrate on the chaotic dynamics of Josephson junction in the presence of applied external ac and dc biasings.

Josephson junction

The tunneling of Cooper pairs through an insulating barrier of a Superconductor-Insulator-Superconductor (SIS) was predicted by B

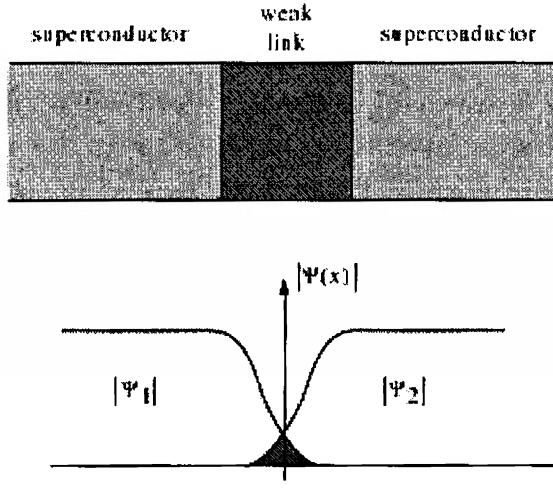


Figure 1.1: The wave function of the superconductor overlapping .

D Josephson in 1962 [2] and experimentally observed by Anderson and Rowell in 1963 [3]. One of the most intriguing properties of Josephson junctions arises from the fact that the dynamics of the charge carriers and the electromagnetic fields in the junction are governed by the phase difference between the quantum mechanical wavefunctions describing the superconducting electrons in the superconductors of the junction. The supercurrent density is not a function of the voltage, but of the phase difference ϕ of the wave functions across the junction:

$$J_s = J_c \sin \phi, \quad (1.2)$$

where J_c , the critical current density is a constant depending on the shape and structure of the junction. The nonlinear properties of this system arises due to the Josephson current which depends on the sine of the phase difference across the junction. The maximum supercurrent density J_c was calculated by Ambegaokar and Bartoff from the microscopic theory and is given as

$$J_c = \frac{\pi}{4} \frac{2\Delta(T)}{\rho e} \tanh\left(\frac{\Delta(T)}{2k_b T}\right), \quad (1.3)$$

where $\Delta(T)$ is the temperature dependent energy gap of the superconductor and ρ is the normal tunnel resistance of the junction per unit area. e is the electron charge and k_b is the Boltzmann constant. Eq. 1.2 is called as the *dc Josephson equation*.

The phase is related to the voltage V developed across the junction by the relation

$$V = \frac{\Phi_0}{2\pi} \frac{d\phi}{dt}, \quad (1.4)$$

where Φ_0 is the flux quantum given as

$$\Phi_0 = \frac{h}{2e} = 2.07 \times 10^{-15} \text{Wb}. \quad (1.5)$$

dc Josephson effect

An interesting feature of Josephson junction is that a dc current flows through the junction even in the absence of any external applied field. This is known as dc Josephson effect. Let ψ_1 and ψ_2 be the probability amplitudes on either side of the junction. The time dependent Schrödinger equation $i\hbar\partial\psi/\partial t = H\psi$ applied to the

probability amplitude gives two equations of motion

$$\begin{aligned} i\hbar \frac{\partial \psi_1}{\partial t} &= \hbar T \psi_2, \\ i\hbar \frac{\partial \psi_2}{\partial t} &= \hbar T \psi_1, \end{aligned} \quad (1.6)$$

where $\hbar T$ gives the transfer interaction across the junction. Depending on the nature of the junction the value of T varies. Substituting $\psi_1 = n_1^{1/2} \exp(j\theta_1)$ and $\psi_2 = n_2^{1/2} \exp(j\theta_2)$ in Eq.1.6 and solving we get an equation for the current flowing through the junction in the absence of the applied voltage as

$$J_s = J_c \sin \phi, \quad (1.7)$$

where $\phi = \theta_1 - \theta_2$. n_1 and n_2 are the Cooper pair densities and $\theta_{1,2}$ are the phase factors of the wavefunction. The value of J_c will depend on the value of T . From Eq. 1.4 it can be seen that for zero voltage there is no rate of change for the phase difference ϕ . Thus in the absence of an external voltage a constant current will flow through the junction which is known as the “dc Josephson effect”.

ac Josephson effect

In the presence of an applied constant voltage V , the equations of motion become,

$$i\hbar \frac{\partial \psi_1}{\partial t} = \hbar T \psi_2 - eV \psi_1, \quad (1.8)$$

and

$$i\hbar \frac{\partial \psi_2}{\partial t} = \hbar T \psi_1 + eV \psi_2. \quad (1.9)$$

In this case substituting the values of $\psi_{1,2}$ and solving we get the expression for the current flowing through the junction as

$$J_s = J_c \sin \left(\phi(0) - \frac{2eVt}{\hbar} \right).$$

The current oscillates with a frequency $\omega = (2eVt)/\hbar$ and thus a constant dc voltage gives an ac current as the output. This is known as the “ac Josephson effect”.

In the presence of an applied ac-biasing the dynamics of the Josephson junction becomes more complex and the system exhibits even chaotic motion.

1.1 Josephson junction model

A Josephson junction shown in Fig.(1.2) consists of two superconducting films separated by an oxide barrier thin ($\sim 10\text{\AA}$) enough for Cooper pairs to tunnel through the barrier. The Josephson junction may be characterized by the current and voltage at the terminals as if it is a two terminal device. The junction may be categorized as short or long junctions depending on the junction area.

1.1.1 Short Josephson junctions

In the case of short Josephson junctions, the variation of the phase difference across the area of the junction may be neglected. This kind of an approximation is valid in cases where the lateral junction dimensions are smaller than the characteristic length scale λ_J of the variation of ϕ . Small Josephson junctions may be modeled using a

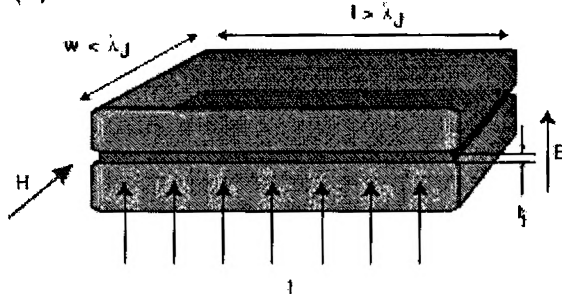


Figure 1.2: The Josephson junction consisting of two superconducting electrodes separated by thin oxide barrier.

resistor capacitor and a Josephson junction current element as shown in Fig 1.3. The junction is represented by a parallel connection of an ideal Josephson junction, a resistor to represent the junction resistance and a capacitor for accounting for the Cooper pair, the quasiparticle and the capacitive contribution of the total current. Using Kirchoff laws the total current through the junction is given by

$$I = I_c \sin \phi + \frac{V}{R} + C \frac{dV}{dt}. \quad (1.10)$$

This model is known as the resistively and capacitively shunted Josephson junction (RCSJ) model [7, 8]. Substituting the value of V from Eq. 1.4 in Eq. 1.10 we get

$$I = I_c \sin \phi + \frac{\phi_0}{2\pi R} \frac{d\phi}{dt} + \frac{\Phi_0 C}{2\pi} \frac{d^2\phi}{dt^2}. \quad (1.11)$$

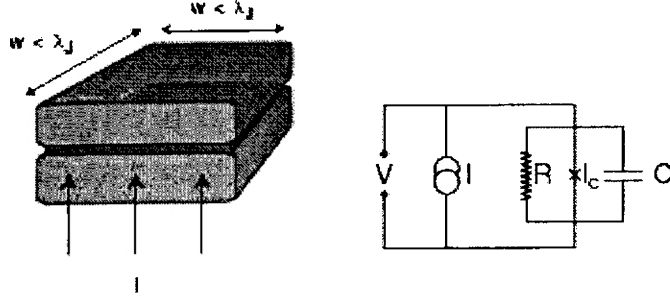


Figure 1.3: Short Josephson junction and equivalent circuit model.

Substituting Eq. 1.5 in Eq. 1.11 we get

$$I = I_c \sin \phi + \frac{\hbar}{2eR} \frac{d\phi}{dt} + \frac{\hbar C}{2e} \frac{d^2\phi}{dt^2}. \quad (1.12)$$

In this thesis, we assume that the Josephson junction is driven by a current source having both dc and ac components,

$$I = I_{dc} + I_0 \sin(\omega t).$$

Here I_{dc} and I_0 are the amplitudes of the dc and rf currents and $\omega = 2\pi f$ is the angular frequency of the rf current source. In the presence of the external biasing and damping, the phase ϕ can have a complex time-dependent behavior. The voltage in this case is taken as the time-average of the evolution of the phase across the junction

$$V = \langle V \rangle = \left\langle \frac{d\phi}{dt} \right\rangle \frac{\Phi_0}{2\pi}.$$

Depending on the value of the bias current and the damping, the

phase can rotate with small amplitude $\phi < 2\pi$, or it can rotate over 2π . If the phase rotates, a dc voltage drop across the junction appears, whereas the average voltage for small oscillations of the phase is zero [9].

The stored energy U as a function of ϕ may be written as

$$U(\phi) = \int I_s V dt = \frac{\hbar I_s}{2e} \int_0^\phi \sin \phi d\phi = E_s (1 - \cos \phi),$$

where $E_s = \hbar I_s / 2e$ is the Josephson coupling energy. The dynamic behavior of a Josephson junction in the Stewart - McCumber model [7, 8] is thus analogous to the motion of a particle in a sinusoidal potential, often called as the washboard potential. The nonlinearity of the system is due to the sinusoidal shape of the potential and the strength of the nonlinearity is determined by the Josephson coupling energy E_J .

Usually a Josephson junction is represented by the simplified dimensionless form of equation. For this, a dimensionless time is defined as $t' = \omega_p t$ where $\omega_p = (2eI_c / \hbar C)^{1/2}$ is the plasma frequency of the junction. With this, Eq. 1.12 becomes

$$\frac{d^2\phi}{dt'^2} + \beta \frac{d\phi}{dt'} + \sin \phi = i_{dc} + i_0 \sin(\Omega t'), \quad (1.13)$$

where $\beta = G (\hbar / 2eI_c C)^2$ is the normalized junction conductance, $\Omega = \omega / \omega_p$ is the bias frequency normalized to the plasma frequency, and $i_{dc} = I_{dc} / I_c$ and $i_0 = I_0 / I_c$ are the amplitudes of the dc and rf bias normalized to the critical current. This form of the normalized equation is used in Chapter 2, Chapter 3 and Chapter 4 to study the

chaotic dynamics and synchronization in Josephson junctions .

1.1.2 Long Josephson junctions

While the Stewart - McCumber model is adequate for most of the situations, there is a limitation for the model as it neglects the spatial dependence of ϕ over the junction area. If the area of the junction is large, then the phase difference ϕ between the superconducting layers will also vary in space and hence the dynamics of large area Josephson junctions is much more rich and diverse than that of the short junctions. The long Josephson junction may be modeled with two small RCSJ-like junctions connected parallelly using an inductance and a resistance as shown in Fig 1.4. Using Kirchoff laws and making necessary normalization, the equation for a long Josephson junction may be given as

$$\frac{\partial^2 \phi}{\partial x^2} + \frac{\partial^2 \phi}{\partial y^2} - \frac{\partial^2 \phi}{\partial t^2} - \sin \phi - \alpha \frac{\partial \phi}{\partial t} = 0, \quad (1.14)$$

where $\alpha = G_s (\hbar/2eJ_c C_s)^{1/2}$. In this case, the junction is characterized by a critical current density J_s , specific conductance G_s and specific capacitance C_s which determine the pair, quasiparticle and displacement currents per unit area. The spatial coordinates are normalized to the Josephson penetration depth as $x = x'/\lambda_j$ and $y = y'/\lambda_j$. λ_j depends on material parameters by the relation $\lambda_j = [2e\mu_0 J_c (s + 2\lambda_L)/\hbar]^{-1/2}$, where μ_0 is the permeability of free space, s is the thickness of the oxide barriers, and λ_L is the London penetration depth of the superconductor. Eq. 1.14 is solved with the boundary conditions that include the appropriate bias currents

in order to study the dynamics of the system.

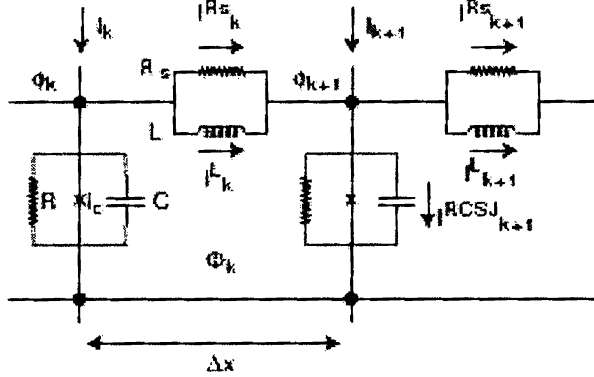


Figure 1.4: Equivalent circuit model for long Josephson junction .

Among these extended Josephson junction systems, the investigation of one dimensional long Josephson junction is of particular interest and a lot of investigation has been done in this direction [9].

Rectangular Josephson junction

The rectangular one dimensional Josephson junction can be modeled by the following equation.

$$\frac{\partial^2 \phi}{\partial x^2} - \frac{\partial^2 \phi}{\partial t^2} - \sin \phi = \gamma + \alpha \frac{\partial \phi}{\partial t}, \quad (1.15)$$

where γ is the applied biasing. The boundary condition for an infinite long linear junction is

$$\frac{\partial \phi}{\partial x}(x = \pm\infty) = 0.$$

If we neglect the perturbations on the R.H.S of Eq. 1.15, the equation becomes the sine-Gordon equation

$$\frac{\partial^2 \phi}{\partial x^2} - \frac{\partial^2 \phi}{\partial t^2} - \sin \phi = 0 \quad (1.16)$$

whose solution is given as

$$\phi_u(x, t) = 4 \arctan \left[\exp \left(\pm \frac{x - ut - x_0}{\sqrt{1 - u^2}} \right) \right]. \quad (1.17)$$

Depending on the sign of the solution, ϕ_u represents a kink or an antikink solution. The kinks in Josephson junctions are examples of solitons. Solitons are solitary waves which exist in media where dispersion and nonlinearity compensate each other leading to stable wave propagation in the media. In Josephson junction systems there is no dynamical restriction in the existence of the solitons and hence they are examples of topological solitons. This is in contrast to the dynamical solitons which need to have certain minimum energy for dispersion to be managed by nonlinearity.

The fluxons (kink solutions) in Josephson junction can be driven by external forces. In the presence of an external magnetic field, the boundary conditions of the rectangular junctions change to

$$\frac{\partial \phi}{\partial x}(x = 0, l) = H,$$

where H is the normalized magnetic field. The interaction of the fluxons with the boundaries strongly influences the dynamics of the fluxon inside the junction. In long Josephson junctions the behavior of the fluxons may be described as follows [10].

Zero-field steps(ZFSs): In the absence of magnetic field, fluxons get nucleated for certain bias current giving rise to ZFSs in the current-voltage characteristic of the junction. The applied bias current drives the fluxon, which changes the polarity after reflecting at the boundary.

Fiske steps(FSSs): If the magnetic field applied to the long linear Josephson junction is above some critical value, fluxons are nucleated at one end and annihilated at the other end of the junction. Upon annihilation, plasma waves are generated which resonates as cavity modes of the long Josephson junction generating the so called Fiske modes.

Flux Flow steps(FFSs): At high magnetic fields resonant Fiske states overlap and the dynamics is purely determined by the flux flow i. e. , a dense chain of fluxons moving unidirectionally through the junction.

Non-rectangular Josephson junction

Non-rectangular Josephson junctions have been in the focus of fluxon dynamics studies in recent years because of the non uniformity caused by the shape. Among the various non-rectangular geometries proposed, the annular Josephson junction has been studied extensively both theoretically and experimentally because the number of fluxons are conserved. An *annular Josephson junction* [9] is formed by two ring shaped superconducting electrodes separated by a thin barrier as shown in Fig 1.5. The equation for an annular junction

may be given as

$$\frac{\partial^2 \phi}{\partial x^2} - \frac{\partial^2 \phi}{\partial t^2} - \sin \phi = b \sin(kx) + \gamma + \alpha \frac{\partial \phi}{\partial t}. \quad (1.18)$$

where $b = B\Delta 2\pi/l$ and $k = 2\pi/l$. Δ is the coupling between the external field B and the flux density of the junction. The annular Josephson junctions are represented by the boundary conditions

$$\phi(x=0) = \phi(x=l) - 2\pi n$$

and

$$\frac{\partial \phi}{\partial x}(x=0) = \frac{\partial \phi}{\partial x}(x=l)$$

where l is the circumference of the junction. n is the number of fluxons initially present in the junction and it is a conserved quantity due to the closed topology of the junction. The second boundary condition enforces the continuity of the magnetic field along the junction. In annular Josephson junctions the motion is smoother as the fluxons cannot collide with the boundaries.

The localized topological solitons can be treated as relativistic pseudo-particles with a center of mass and momentum. They also carry magnetic moment which causes an interaction with external magnetic field. The magnetic moment is always normal to the junction. Therefore, by shaping the junction, a suitable potential for these pseudo-particles can be formed. Among the other non-rectangular shaped Josephson junctions, the *heart shaped junction* has been found to be an ideal candidate for quantum computation because of the double well shaped potential of the system. The junc-

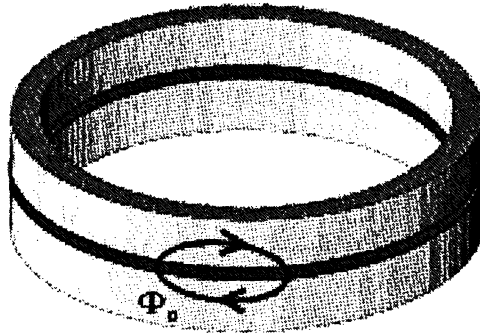


Figure 1.5: Annular Josephson junction model.

tion composed of a large arc, which corresponds to half an annular junction. Then two small arcs were connected at the top to form a heart shaped junction [11]. It was shown by Kemp et al. [11] that a double well potential can be created in a heart shaped Josephson junction and it can be effectively used as a qubit. Considering this idea Josephson junctions with other shapes like *semiannular*, *quarter annular* and *S-shaped* junctions were put forward by Shaju et al. [12, 13, 14]. Among these, semiannular Josephson junction was shown to have immense applications. The semiannular shape creates opposite polarities at the ends of the junction making it an ideal candidate for the realization of Josephson junction based diodes. It was also shown to have characteristics which makes it find applications as magnetic rectifiers, oscillators etc. S-shaped Josephson junction was found to have a double well potential making it ideal for Josephson junction based qubits. In Chapter 5 of this thesis, we discuss in

detail the dynamics of fluxon in a semiannular Josephson junction in the presence of a magnetic field. .

1.2 Chaos

Chaos is the phenomenon of occurrence of bounded nonperiodic evolution in completely deterministic nonlinear dynamical systems with high sensitive dependence on initial conditions [15]. It is a characteristic property of nonlinear systems. A dynamical system may be defined as a deterministic mathematical prescription for evolving the state of a system forward in time. Dynamical systems are normally regulated by system parameters and the change in the values of the system parameter is reflected in the behavior of the system. Even though all dynamical systems evolve according to some deterministic set of equations, the behavior becomes unpredictable for some parameter values. The only uncertainty in such systems is in the long term predictability of the system.

Nonlinear differential equations are in general difficult to solve analytically and there are no general ways to solve them as in the case of a linear equations [16]. The linear systems can be broken to parts and each part may be solved separately and all may be recombined to get the final answer. Also, methods like Laplace transform, Fourier analysis and superposition principle may be applied in the case of linear differential equations. But there are no such general methods for the nonlinear systems. However, there are alternative ways to study the dynamics of systems without analytically finding out the solutions. Chaotic dynamics rely heavily on these “geomet-

ric methods” for gathering information about the dynamics of the system as analytic solutions do not exist in the chaotic regime. If we know the position and velocity at a particular instant of time, we can construct the trajectory in the *phase space* representation without actually solving analytically the equation of motion. A great amount of information may be gathered from the trajectories constructed.

For a continuous dynamical system, the necessary number of degrees of freedom for observing chaos is three or more though there is no such restriction in the case of discrete maps. Maps may be defined as dynamical systems represented by discrete time-difference equations and a general form may be given as

$$\vec{X}_{n+1} = F_{\mu}(\vec{x}_n) \quad (1.19)$$

where μ is the control parameter. Consider a system represented by n differential equations

$$\dot{x}_1 = f_1(x_1, \dots, x_n) \quad (1.20a)$$

$$\vdots$$

$$\dot{x}_n = f_n(x_1, \dots, x_n) \quad (1.20b)$$

where the overdots represent differentiation with respect to time t . The phase space for such a system is the space with coordinates x_1, \dots, x_n and hence is an n dimensional space. Given the initial conditions, for a deterministic system we can find the trajectory at a later instant.

In the case of nonautonomous system (ie. system with explicit

time dependence) time is taken as the last variable. For example, if there is a second order nonautonomous differential equation by taking the third variable as time, the system can be represented by an equivalent three dimensional system. Hence a second order differential equation with an external drive exhibits chaotic dynamics.

1.2.1 Ways to characterize chaos

The identifying characteristics of a chaotic system is that its occurrence is neither due to the uncontrolled external forces like noise nor due to the large number of degrees of freedom, but because of the inherent nonlinearity associated with the system that induces the sensitivity to initial conditions.

Sensitive dependence to initial conditions: The main feature of chaotic dynamics is its extreme sensitive dependence to initial conditions. Considering two trajectories $x_1(t)$ and $x_2(t)$ starting from nearby initial conditions separated by δ , it can be seen that for a chaotic system the difference between the trajectories $\Delta = x_1(t) - x_2(t)$ grows exponentially with time. However, the orbit should remain bounded for the system to be characterized as chaotic. Due to the exponential sensitivity to the initial conditions, small errors in the solution can grow very rapidly with time. Hence effects such as noise and computer round off can totally change the solution from what it would have been in the absence of these effects. All these make the long term predictability of chaotic system completely impossible in a practical sense. An important question which arises in this context is whether the trajectory obtained by numerical simulation is an artifact of the chaos amplified by computer roundoff?

By rigorous mathematical proof of the shadowing property of certain chaotic systems it was shown that although a numerical trajectory diverges exponentially from the true trajectory with the same initial condition, there exists a true trajectory with slightly different initial conditions that stays near the numerical trajectory [17, 18, 19].

Poincaré maps: Poincaré maps are a method used to construct a discrete mapping of a deterministic dynamical system which is originally described by nonlinear differential equations. Let $\dot{x} = f(x)$ represent an n dimensional system and S be an $n - 1$ dimensional surface of section defined such that all trajectories starting on S will flow through it and not parallel to it. The Poincaré map P is a mapping from S to itself and is obtained by following the trajectories from one intersection with S to the next [20]. Consider a three dimensional phase plane where we define a section S in the two dimensional plane. The trajectories are followed and marking is made when the trajectory crosses the section in the same direction. The points obtained by this method constitute the Poincaré section and the points will be related to each other as $P_{n+1} = f(P(n))$, where f is a nonlinear function. Thus taking a Poincaré section reduces the dimension of the system. In cases where the system is driven by a periodic force, say $f \cos(\omega t)$, the points are picked at intervals of $t_n = n2\pi/\omega + t_0$ where n is an integer, $2\pi/\omega$ is the period of the driving force and t_0 is arbitrary [15].

Bifurcation: When the value of a system parameter is changed, the qualitative properties of the attractor of a dynamical system may get changed. The motion may change from periodic to quasiperiodic or to chaotic taking different routes. An abrupt qualitative change of

this kind is called a bifurcation. During bifurcation, an attractor may appear, disappear or one attractor may be replaced by another one. Bifurcation diagrams help us to view these transitions. They are the plots of attractor points versus the system parameter values which cause these transitions. The onset of chaos is usually associated with a few types of bifurcation [20, 21]. For plotting the bifurcation of continuous dynamical systems, a set of values of a single variable representing the attractor must be obtained. One way to do this is by taking the return map from the Poincaré section. There is another method for obtaining discrete mapping from the flow. Lorentz constructed a one dimensional map from the three dimensional flow by taking the consecutive maxima of a single variable and plotting it against the system variable [22]. In this thesis, we plot bifurcation by taking the maxima of the time series and plotting the values against the parameter. So for a particular parameter value, if the motion is single periodic it will correspond to a single point in corresponding bifurcation plot. As the parameter value is increased the number of points increases depending on the change of the motion to doubly periodic or chaotic.

Lyapunov exponents: The Lyapunov exponents are a convenient indicator of the sensitivity to the small orbit perturbations of the chaotic attractors. They quantify the average exponential rate of divergence of nearby orbits. A positive Lyapunov exponent implies chaotic motion. In order to define the Lyapunov exponent, consider the nonlinear continuous differential equation

$$\frac{dx(t)}{dt} = F(\mathbf{x}(t)), \mathbf{x} \in \mathbb{R}^N \quad (1.21)$$

where $F(\mathbf{x}(t))$ is a nonlinear function of vector $\mathbf{x}(t)$ representing the state variables given by $\mathbf{x} = (x_1, x_2, \dots, x_n)$. Let $\mathbf{x}(0)$ represent the initial condition at which a solution $\mathbf{x}(t)$ exists. Consider another trajectory starting from a nearby initial point $\mathbf{x}(0) + \delta\mathbf{x}(0)$. If $\delta\mathbf{x}(t)$ is the separation between the trajectories after a time t , then the Lyapunov exponent may be defined as [21]

$$\lambda(\mathbf{x}(0), \delta\mathbf{x}(0)) = \lim_{t \rightarrow \infty} \frac{1}{t} \log \frac{\|\delta\mathbf{x}(t)\|}{\|\delta\mathbf{x}(0)\|}. \quad (1.22)$$

In order to evaluate the Lyapunov exponents numerically, different algorithms are followed out of which the algorithm by Wolf et al. is the commonly used one [23].

Numerical methods: Most of the nonlinear equations are not exactly solvable. Even in cases where exact solutions are obtained, it may involve many integrals or infinite series making it virtually useless. So mostly we rely on computer simulations to find the form of the solution. By using step-by-step method on a computer, most of the equations may be solved numerically. However, for nonlinear equations that could not be solved analytically, there is no rigorous method to make certain that these simulations are faithful to the equations. The only way to make sure is that the simulated system must agree for cases where any analytic solution is known and the systems simulated by different numerical methods should agree. In order to solve second order differential equation we use the fourth order Runge-Kutta method.

Runge-Kutta method: Numerical approximation to a solution to any first order differential equations depends on the Taylor series

approximation. In principle one can get the value of a function at a value $y(x_n + h)$, if we know the value of the function as well as its derivatives at x_n where h is the step size. All available methods are different in the way by which they choose the order of truncating the Taylor series at various order in the powers of the step size h . We categorize them according to various order in the powers of the step size h . First is the Euler's method where linear approximation is used to find the value of the function at $x_n + h$. For this method the requirement is the value of the function at x_n and the slope of the function. In this case truncation is at the first order and error is $O(h^2)$. From second order onwards we can see various methods which differ from each other in calculating the slopes. These different methods come under the big family called Runge-Kutta methods, and they are infinite in number for each order. It is for the users to choose among them, each one having its own merits and demerits. The general expression for the value of the function at $x + h$ is

$$y(x + h) = y(x) + \text{Average of the slopes} \times h.$$

In order to get the accuracy, we add higher and higher orders in h , which make the numerical evaluation cumbersome. Thus a compromise should be made between accuracy and time for evaluation. It was observed that taking these into consideration, the 4th order Runge-Kutta expression was more appropriate for the usual situations, which in fact is called as 'the classic Runge-Kutta formula'. This has the form

$$y_{n+1} = y_n + h \times (k_1 + 2k_2 + 2k_3 + k_4)/6 \quad (1.23)$$

where

$$\begin{aligned}
 k_1 &= f(x_n, y_n) \\
 k_2 &= f\left(x_n + \frac{1}{2}h, y_n + \frac{1}{2}k_1\right) \\
 k_3 &= f\left(x_n + \frac{1}{2}h, y_n + \frac{1}{2}k_2\right) \\
 k_4 &= f(x_n + h, y_n + k_3).
 \end{aligned}$$

Here k 's are the average of slopes and $x_{n+1} = x_n + h$.

1.3 Different routes to chaos

As discussed in Section 1.2.1, depending upon the system parameter values the dynamics may change from periodic to chaotic. There are several routes through which a dynamical system enter a chaotic regime as revealed by bifurcation diagrams. The common routes to chaos are period doubling route, quasiperiodic routes and intermittency. In the period doubling or Feigenbaum route to chaos, as the value of the control parameter is varied, a stable fixed point becomes unstable and a new set of two fixed point appears. As the parameter value changes, this process repeats and for some values of parameter the system becomes chaotic. The phenomenon where a set of 2^n fixed points in the phase space of a system disappears and a new set of 2^{n+1} fixed points arise is called a period doubling bifurcation or a pitchfork bifurcation. Instead of this mechanism, there is another case where the stable fixed points bifurcate into a limit cycle at some critical value of control parameter. This is known as Hopf bifurcation [24]. The basic mechanism in the quasiperiodic or Ruelle-

Takens route to chaos is the Hopf bifurcation. The Hopf bifurcation is followed by a transition to a double periodic torus and this torus bifurcates into a chaotic attractor having fractal dimensions [25]. In the intermittent route to chaos, the dynamics is characterized by alternate bursts of chaotic behavior and almost periodic oscillations.

1.3.1 Chaos in Josephson junctions

A major field in the physics of Josephson junction is concerned with the classical non-linear electrodynamics of small junctions, arrays of small junctions and extended junctions. If the Josephson junction were a linear device, then a periodic forcing would yield a steady-state solution having the same period as the rf bias. The sine term in Eq. 1.2 makes Josephson junction a nonlinear system and hence quasiperiodic or chaotic attractors may be expected in it. Due to the nonlinearity, the junction phase may fail to synchronize with the rf bias and advance by a regular amount during each rf cycle. Such solutions are said to be quasiperiodic. There is also a possibility that the steady state motion includes a pseudorandom component and this state is referred to as chaotic [26]. Though the first system in which chaos was mathematically established by Poincare [27] had equations similar to that of an undamped Josephson junction, the recognition of chaos in Josephson junction was raised by Belykh et al. in 1977 [28]. Chaos in Josephson junction (JJ) has been studied extensively after its presence was demonstrated using numerical simulation [29]. The rf-biased JJs find practical importance in the construction of devices like parametric amplifiers, voltage standards, pulse generators, SQUID for detection of very weak magnetic fields, etc. [30, 31, 32].

JJs consisting of Superconductor-Insulator-Normal metal-Insulator-Superconductor (SINIS) showing non-hysteretic I-V characteristics with high damping has been fabricated for programmable dc-voltage standards [33] or ac-voltage standards based on synthesis of calculable wave forms[34]. For these devices, it is essential to avoid all types of noise, chaos etc. Devices like voltage standards [35] which rely on nonlinearity to create a phase lock between the internal junction variable and an applied rf bias, has an optimum operating point in regions near chaos. Understanding of the onset of chaotic behavior is very crucial in understanding the stability of an rf-biased junction.

Eq. 1.12 describing the behavior of JJ is identical to the equation for a driven damped pendulum which has been studied theoretically for several routes to chaos[36, 37]. Sullivan and Zimmerman constructed such a mechanical analogue and measured average rotation as a function of applied torque which is the analogue of the I-V curve of Josephson junctions. In the mechanical analogue, junction voltage is represented by particle velocity, bias currents are represented by external forces, the junction capacitance becomes particle mass, and the junction conductance $G = 1/R$ translates into viscous damping. From Eq. 1.13 it is clear that the dynamic properties of an rf biased Josephson junction depends on four parameters, β , Ω , i_{dc} and i_0 . So an important goal in the study of Josephson junction dynamics is to determine the ranges of these parameters over which the system is chaotic.

In Josephson junction systems, the state space ordinarily requires two state variables (ϕ and $v = d\phi/dt'$). If a time-dependent bias is present, then time is taken as the third variable by defining $z = \Omega t'$

in Eq. 1.13. Thus the rf biased system may be considered as time-invariant on a three dimensional state space. The minimum dimension required for a continuous system to exhibit chaos is three and hence the rf-biased Josephson junction is among the simplest systems to exhibit chaos. Lyapunov exponents for the chaotic solutions for the rf-biased Josephson junction were first computed by Steeb et al. [38]. Since the rf-biased Josephson junction does not have any fixed points, one of the three Lyapunov exponents is always zero. It was shown by Kautz [39] that as the state-space volume always shrinks, it implies the sum rule

$$\lambda_1 + \lambda_2 = -\beta$$

where λ is the Lyapunov exponent .

1.4 Synchronization of chaotic systems

Synchronization is an adjustment of rhythms of oscillating objects due to their weak interaction. The colloquial meaning of synchronization is “agreement or correlation of time in different processes”. It was an active topic of research since the time of Huygens [42]. Huygens noticed that two weakly coupled pendula get synchronized in phase. However, identification of synchronized motion in chaotic systems was indeed surprising as chaotic systems are very sensitive to initial conditions. Hence the natural tendency of two chaotic systems coupled together will be to defy synchronization as the trajectories starting with nearby initial conditions will diverge in phase space. Therefore synchronization among such systems is of great impor-

tance and interest. Since it was shown that chaotic systems could be synchronized by linking them to a common signal [43, 44], many works have been done in this direction because of its applications in secure communication [45].

The coupling configuration is very important while considering synchronization of systems. Pecora and Carroll demonstrated that chaotic systems could be synchronized with unidirectional coupling in a master-slave model [46]. In this type of coupling one subsystem (drive) evolves freely and drives the evolution of the other. Here the slave system is forced to follow the dynamics of the drive system which is chaotic. In the area of communication with chaotic systems this kind of coupling is used. The second type of configuration is the bidirectional coupling where both the subsystems are coupled to each other and the coupling factor induces an adjustment of rhythm into a common synchronization manifold, thus inducing mutual synchronization behavior [47]. Typical examples are the interaction between neurons or between lasers with a feedback in between. The result due to the two types of coupling are different and interesting in their own ways.

In an attempt to provide a unified definition for different kinds of synchronizations the following definition was given by Brown et al. [49].

The subsystem given by

$$\dot{x} = f_1(x; y; t); \quad \dot{y} = f_2(y; x; t)$$

are synchronized on the trajectory $k(z_0)$, with respect to the proper-

ties, g_x and g_y , if there is a time independent mapping $h : R^k \otimes R^k \rightarrow R^k$ such that

$$\|h[g(x), g(y)]\| = 0,$$

where $\|\cdot\|$ is the norm. Here the time-dependent function $h : R^k \otimes R^k \rightarrow R^k$ compares the measured properties of the two subsystems, and the two measurements agree in time if and only if $h[g(x), g(y)] = 0$. $k(z_0)$ is the trajectory of the total system which can be separated into $k_x(z_0)$ and $k_y(z_0)$ of the smaller subsystems. g_x is the property that we measure of the first subsystem. In the above definition for synchronization, the details of initial conditions are also present. In the case of chaotic synchronization, it depends strongly on the trajectory. While two subsystems may synchronize on one trajectory, the same subsystem may not synchronize on another trajectory. However the problem about the stability of synchronization is not included in the above definition. Hence a second definition is given as [49]

the subsystem given by

$$\dot{x} = f_1(x; y; t); \quad \dot{y} = f_2(y; x; t)$$

are synchronized with respect to the properties g_x and g_y , if there is a time independent mapping $h : R^k \otimes R^k \rightarrow R^k$ such that

$$\|h[g(x), g(y)]\| = 0$$

holds on all trajectories. This definition demands that if there is a small perturbation from one trajectory still the condition $\|h\| = 0$

holds good and hence it takes into account of the stability of the synchronized state.

In the following sections, we discuss the various types of synchronization in detail.

Complete synchronization

For identical systems, synchronization may appear as the equality of state variables while evolving in time. This condition is referred to as complete synchronization or identical synchronization. In this kind of synchronization the properties of the subsystem are the phase variables themselves i.e $g(x) = x(t)$ and $g(y) = y(t)$. In complete synchronization the chaotic trajectories of the subsystems remain in step with each other for the entire course of time. This kind of synchronization was first shown to occur in two unidirectionally coupled systems [46]. All the conditional Lyapunov exponents of the synchronized subsystems would be negative. This type of synchronization is also referred to as conventional synchronization [50]. Complete synchronization is exhibited by systems with both unidirectional and bidirectional coupling. The appearance and robustness of the synchronization states for different coupling schemes have been discussed in references [51, 52, 53].

Complete synchronization may be achieved in identical systems which are properly coupled. However, in real physical systems there may be parameter mismatches and hence the systems are not identical. Complete synchronization may not occur in such cases as there does not exist an invariant manifold $x = y$.

Frequency synchronization

Frequency is the subsystem property which we measure in this synchronization. Measuring a property indicates that we are calculating a numerical value for that property. So in this case g_x is the property being measured and the numerical value $g_x = \omega$ is the frequency. In frequency synchronization comparison is made between properties that are time averages on the trajectory. Hence in this kind of synchronization there is no restriction on the instantaneous values of the coordinates x and y [49].

Phase synchronization

For unsynchronized chaotic oscillators, as the coupling strength is gradually increased, a weak degree of synchronization referred to as phase synchronization may occur, where the suitably defined phases of the chaotic oscillators become locked, while the amplitudes remain uncorrelated. In order to define the “phase” of a chaotic system different methods are used. If the dynamics is chaotic and phase coherent one way is to define the phase as the angle coordinate $\varphi(t)$. Another method is to define the phase by a Hilbert transform in cases where the phases are not uniquely defined on the subsystem [48]. Phase synchronization compares only the phase variables. Hence in this state the amplitudes can remain relatively uncorrelated.

The two kinds of synchronization described above can be included in the definition for synchronization as the definition depends on the property of the subsystem that we measure and not on the difference between the variables $\|x - y\|$ as most of the definitions do.

If the chaotic oscillations cover a broad range of time scales, the phase will not completely synchronize, but will have intermittent phase slips. This is known as imperfect phase synchronization[54].

Lag synchronization

As the coupling strength is increased further, the synchronization becomes stronger with even the amplitudes getting correlated, but with a proper shift in time. This is known as lag synchronization and in this case the properties measured lag behind each other by a fixed time, τ . In order to characterize lag synchronization quantitatively, similarity function is used which is discussed in detail in Chapter 2. With strong enough coupling, the time lag may become zero and the two systems may become completely synchronized [47].

Generalized synchronization

For strong enough coupling the dynamics of the system represented by $\dot{x} = f_1(x)$ and $\dot{y} = f_2(y)$ is constrained to a subspace in the whole phase space of the system (\mathbf{x}, \mathbf{y}) . But as it is non-identical systems this subspace is not the $\mathbf{x}=\mathbf{y}$, but defined by a more complicated functional relationship between them. This hidden synchronization is known as generalized synchronization [55, 56].

1.4.1 Stability of synchronization

Consider a system represented by the variables x_1, x_2, x_3 coupled to a second system with variables y_1, y_2, y_3 . In a drive response system y_1 can be replaced by x_1 and under suitable conditions after a

long time we may get the two equalities $x_2 = y_2$ and $x_3 = y_3$. This condition is identical synchronization and it restricts the motion of the system to a lower dimensional hyperplane. In general, when systems are synchronized, the phase space trajectories of the combined system are confined to a low dimensional hyperplane called synchronization manifold. The coordinates of the space orthogonal to the synchronization manifold should be zero if the motion is in the synchronization manifold. The stability of the synchronized state depends on the property whether the system is attracted to that manifold when started away from it. The minimal condition for the stability of the synchronized state is that the Lyapunov exponent associated with the equation for the space transverse to the synchronization manifold should be negative [51, 57].

1.5 Outline of the thesis

The main goal of this thesis is to study the dynamics of Josephson junction system in the presence of an external rf-biasing. A system of two chaotically synchronized Josephson junction is studied in **Chapter 2**. The change in the dynamics of the system in the presence of a phase difference between the applied fields is considered. Control of chaos is very important from an application point of view. The role of phase difference in controlling chaos is discussed. **Chapter 3** is an extension of the work presented in the previous chapter for an array of N Josephson junctions. An array of three Josephson junctions is studied for the effect of phase difference on chaos and synchronization and the argument is extended for a system of N Josephson

junctions. In the presence of a phase difference between the external fields, the system exhibits periodic behavior with a definite phase relationship between all the three junctions. **Chapter 4** deals with an array of three Josephson junctions with a time delay in the coupling term. It is observed that only the outer systems synchronize while the middle system remain uncorrelated with the other two. The effect of phase difference between the applied fields and time-delay on system dynamics and synchronization is also studied. In **Chapter 5** we study the influence of an applied ac biasing on a semiannular Josephson junction. It is found the magnetic field along with the biasing induces creation and annihilation of fluxons in the junction. The I-V characteristics of the junction is studied by considering the surface loss term also in the model equation. The system is found to exhibit chaotic behavior in the presence of ac biasing. In **Chapter 6**, the results are briefed and the future plan of work is also presented

Chapter 2

Suppressing chaos in coupled Josephson junctions

2.1 Introduction

The interaction of Josephson junctions(JJ) with external fields plays important roles in the development of physics and chaotic dynamics of JJs [58, 59, 60, 61]. The existence of chaos in rf-biased JJ has been verified through theory, numerical simulation and experiments [62]. Control of chaos continues to be an active area of research [40] because of the many undesirable effects chaos brings in mechanical systems and other devices. By controlling chaos in rf-biased JJs, it was shown that even in the presence of thermal noise, they could be used as voltage standards [63]. Suppression of temporal

and spatio-temporal chaos allows complex systems to be operated in highly nonlinear regimes. This is required in many physical systems. Most of the Josephson junction devices are made of more than one junction coupled together. Depending upon the values of the parameters, these coupled Josephson junctions may exhibit both periodic and chaotic motion. It becomes necessary to control chaos in such systems for obtaining optimum working condition. For example, it was shown that the optimum working condition for Josephson junction based voltage standards are near the region of chaos [39]. Thus the study of these nonlinear systems in the chaotic regime comes of practical importance.

2.1.1 Coupled Josephson junctions

In this chapter, we consider the dynamics of two short Josephson junctions in the presence of applied external biasing. The equations for the short Josephson junction may be given by the RCSJ [7, 8] model described in Section 1.1.1. Each junction is characterized by the phase difference ϕ_i between the order parameters representing the superconducting state, a critical current i_{ci} , capacitance C_i and normal resistance R_i with $i = 1, 2$. There are two ways by which such junctions may be coupled.

Parallely connected Josephson junctions

The coupled Josephson junctions consists of a pair of junctions wired in parallel with a linking resistor R_s . The resistor R_s provides the coupling between the junctions. Schematic representation of the sys-

tem is given in Fig(2.1). 1 and 2 represent the applied external fields. The dynamical equations can be written by using the Kirchoff law

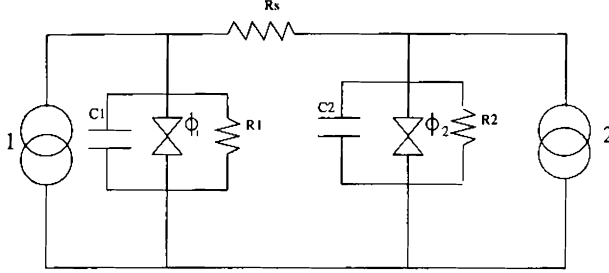


Figure 2.1: Schematic representation of a coupled Josephson junction connected in parallel with a linking resistor R_s . 1 and 2 represents the applied fields.

as

$$\frac{\hbar C_1}{2e} \frac{d^2 \phi_1}{dt'^2} + \frac{\hbar}{2eR_1} \frac{d\phi_1}{dt'} + i_{c1} \sin \phi_1 = i'_{dc} + i'_0 \cos(\omega t') - i_s \quad (2.1)$$

$$\frac{\hbar C_2}{2e} \frac{d^2 \phi_2}{dt'^2} + \frac{\hbar}{2eR_2} \frac{d\phi_2}{dt'} + i_{c2} \sin \phi_2 = i'_{dc} + i'_0 \cos(\omega t' + \theta) + i_s, \quad (2.2)$$

where i_s is the current flowing through the coupling resistor and is given as

$$i_s = \frac{\hbar}{2eR_s} \left[\frac{d\phi_1}{dt'} - \frac{d\phi_2}{dt'} \right]. \quad (2.3)$$

In order to express Eqs.(2.1) and (2.2) in dimensionless form the junction plasma frequencies ω_{J1} and ω_{J2} given by $\omega_{J1} = (2ei_{c1}/\hbar C_1)^{\frac{1}{2}}$ and $\omega_{J2} = (2ei_{c2}/\hbar C_2)^{\frac{1}{2}}$ are introduced. The normalized time scale is written as $t = \omega_{J1} t'$. The dimensionless damping

parameter β is defined as

$$\beta = \frac{1}{R_1} \sqrt{\frac{\hbar}{2ei_{c1}C_1}}.$$

The dc bias current i'_{dc} and the rf amplitude i'_0 are normalized to the critical current i_{c1} . The actual frequency ω is re-scaled to $\Omega = \omega/\omega_{J1}$ and the coupling factor is defined as

$$\alpha_s = \frac{R_1}{R_s} \beta.$$

For identical JJs, Eqs.(2.1) and (2.2) can be written as

$$\begin{aligned} \ddot{\phi}_1 + \beta\dot{\phi}_1 + \sin \phi_1 &= i_{dc} + i_0 \cos(\Omega t) - \alpha_s [\dot{\phi}_1 - \dot{\phi}_2], \\ \ddot{\phi}_2 + \beta\dot{\phi}_2 + \sin \phi_2 &= i_{dc} + i_0 \cos(\Omega t + \theta) - \alpha_s [\dot{\phi}_2 - \dot{\phi}_1]. \end{aligned} \quad (2.4)$$

It can be seen that the coupling arises as a natural consequence of the exchange of current through the resistor R_s and it depends on the differential voltage ($\psi_1 - \psi_2$). For JJ devices, phase derivatives are of central importance because they are proportional to junction voltages.

Series-connected Josephson junctions

The Josephson junctions may also be coupled in series with a linking resistor R_s to a common bias as shown in Fig.2.2[73, 74]. The equations for the phase variables now becomes

$$\frac{\hbar C_1}{2e} \frac{d^2 \phi_1}{dt'^2} + \frac{\hbar}{2eR_1} \frac{d\phi_1}{dt'} + i_{c1} \sin \phi_1 = i'_{dc} + i'_0 \cos(\omega t') - i_s \quad (2.5)$$

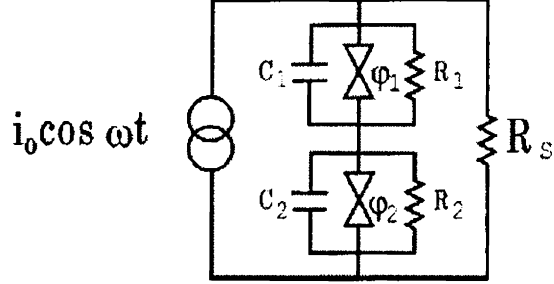


Figure 2.2: Schematic representation of a coupled Josephson junction connected in series.

$$\frac{\hbar C_2}{2e} \frac{d^2 \phi_2}{dt'^2} + \frac{\hbar}{2eR_2} \frac{d\phi_2}{dt'} + i_{c2} \sin \phi_2 = i'_{dc} + i'_0 \cos(\omega t' + \theta) - i_s, \quad (2.6)$$

where i_s is the current flowing through the shunt resistor and is given as

$$i_s = \frac{\hbar}{2eR_s} \left[\frac{d\phi_1}{dt'} + \frac{d\phi_2}{dt'} \right]. \quad (2.7)$$

In this case instead of the difference, it is the sum of the voltages that comes into play.

In this thesis we deal with parallelly connected Josephson junction systems. In order to study the system numerically Eqs.(2.4) is

written in the first order differential form as

$$\begin{aligned}
\dot{\phi}_1 &= \psi_1, \\
\dot{\psi}_1 &= -\beta\psi_1 - \sin \phi_1 + i_{dc} + i_0 \cos(z) - \alpha_s [\psi_1 - \psi_2], \\
\dot{z} &= \Omega, \\
\dot{\phi}_2 &= \psi_2, \\
\dot{\psi}_2 &= -\beta\psi_2 - \sin \phi_2 + i_{dc} + i_0 \cos[(z) + \theta] - \alpha_s [\psi_2 - \psi_1].
\end{aligned} \tag{2.8}$$

where $z = \Omega t$. Eq. (2.8) is studied using fourth order Runge-Kutta method. The time grid is set as 0.005 and it is checked for different values of Δt . The maxima of the time series is plotted. In order to eliminate the transients, the first 50,000 iterations are left out. Also random initial conditions are given. The nonlinear equations are numerically integrated using fourth order Runge-Kutta method as given in Appendix A.1. The values of the system parameters are fixed as $\beta = 0.15$, $i_0 = 0.7$, $i_{dc} = 0.3$ and $\Omega = 0.6$ for numerical simulation.

2.1.2 Lyapunov exponents

A positive Lyapunov exponent indicates chaos. There are different algorithms developed by several authors to determine the complete set of Lyapunov exponent from a set of differential equations. For the numerical evaluation of the Lyapunov exponents, they are defined by the long-term evolution of the axes of an infinitesimal sphere [75, 76].

Then Lyapunov exponents are given by as

$$\lambda_i = \lim_{t \rightarrow \infty} \frac{1}{t} \log_2 \frac{p_i(t)}{p_i(0)} \quad (2.9)$$

where p_i is the length of the ellipsoid principal axis. If we consider the evolution of an infinitesimal n -sphere of initial conditions which represents a continuous dynamical system in an n -dimensional phase space, the sphere will become an n -ellipsoid due to the locally deforming nature of the flow. A well defined direction cannot be associated with the Lyapunov exponent as the orientation of the ellipsoid changes continuously with the evolution. For implementing this method the principal axes are defined with initial conditions whose separations are small as computer limitations allow. The main drawback of this approach is that in a chaotic system the condition of small separations for the times on the order of hundreds of orbital periods needed for the convergence of the spectrum cannot be guaranteed. This problem is avoided in the algorithm developed by Wolf et al. [23]. A fiducial trajectory is created by integrating the nonlinear equations of motion for some post-transient initial conditions. The arbitrarily oriented n orthonormal vectors are defined by simultaneously integrating the linearized equations of motion. Gram-Schmidt orthogonalization procedure is applied on the vector frame to overcome the collapse toward a common direction caused by finite precision of computer calculation. The rate of growth of the first k principal axes is obtained from the projection of the evolved vectors onto the new orthonormal frame. This provides an estimate of the k largest Lyapunov exponents. We follow the algorithm by

Wolf et al. to compute the Lyapunov exponent spectrum. Fig. 2.3 is Lyapunov exponent spectrum plotted against the coupling strengths corresponding to Eq.2.8. We observe that the maximum Lyapunov exponent is positive for all values of coupling strength and it remains at the same positive value. Hence the system exhibits chaotic behavior for all values of coupling strength in the parameter range we selected.

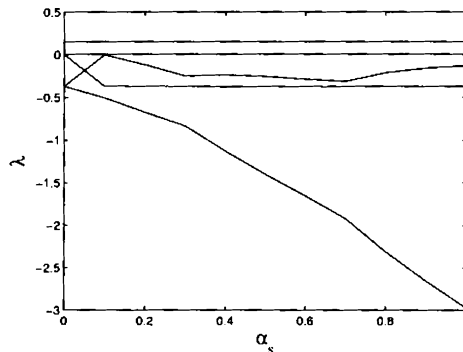


Figure 2.3: Lyapunov exponent spectrum is plotted for different values of coupling strength α_s with $\theta = 0$, $\beta = 0.15$, $i_0 = 0.7$ and $\omega = 0.6$. It can be seen that the system is in chaotic motion for all values of coupling strength.

2.2 Synchronization of Josephson junctions

Since Josephson junction is one of the simplest nonlinear systems to exhibit chaos which can also be verified experimentally, it has been studied both numerically and experimentally for various aspects of the dynamics [26, 29]. Synchronization in JJs has been an interesting

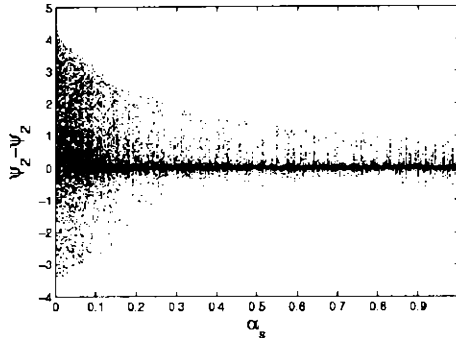


Figure 2.4: Maxima of the difference in voltage against coupling strength α_s . $\theta = 0$, $\beta = 0.15$, $i_0 = 0.7$ and $\omega = 0.6$.

area of research [64, 65]. The studies on synchronizing arrays of Josephson junction has gained momentum since these are identified as sources of electromagnetic radiation in the tertrahertz range. In an array of Josephson junctions, when all the junctions oscillate in phase, the total emitted power is expected to be proportional to the square of the total number of junctions in the array. However desynchronization leads to dramatic drop in emission power. The major challenge arising in this context is to synchronize Josephson oscillations in all junctions in the stack to get significant radiation out of the crystal. There are many methods suggested to bring about synchronization in such arrays. One way is to couple the junctions with resonant cavity and this has been proved efficient both experimentally[66, 67] and numerically [68, 69]. Another popular way is to apply a magnetic field along the junction [70]. Blackburn et al. studied the intermittent chaotic synchronization in a system of

two coupled Josephson junctions [71].

The robustness of synchronization of chaotic systems is of current interest because of its application in secure communication. It is seen that synchronization could be lost even due to small parameter mismatches. In the case of Josephson junctions, even junction capacitances which are often ignored are seen to affect synchronization [72]. A phase difference between the applied fields is found to desynchronize a synchronized system. The effect of phase difference on a system of mutually coupled oscillators was studied by Yin et al. [95]. It is observed that a phase difference destroys synchronization in chaotic oscillators and even brings in lag synchronization. In

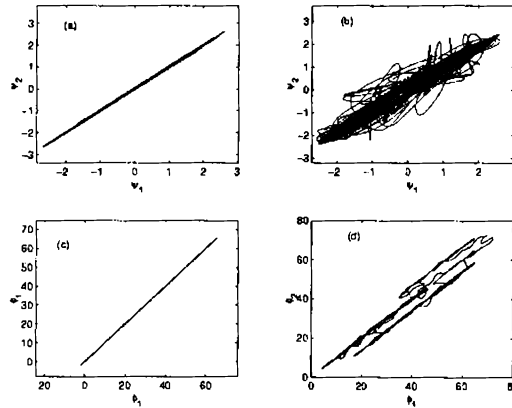


Figure 2.5: a and c show the system is synchronized for $\theta = 0$, $\beta = 0.15$, $i_0 = 0.7$, $i_{dc} = 0.3$, $\alpha_s = 0.45$ and $\omega = 0.6$. b and d show the system desynchronized for a phase difference of $\theta = 0.1\pi$

the system we considered, for large values of coupling strength, it is observed that the difference between the variables of the two systems get smaller. For a complete synchronized state it is expected

that $(\psi_1 - \psi_2)$ should be equal to zero. But in real practical cases there will always be a small $|(\psi_1 - \psi_2)| < \delta$ which can be associated with synchronization. The value of δ varies from systems to systems. Fig. 2.4 shows the variation in the difference between the voltage against the coupling strength. It can be observed that as the coupling strength is increased the difference between the variables decreases drastically. From the various coupling strength values we chose $\alpha_s = 0.45$ as the system exhibited perfect synchronization in this region. This can be observed from Figs. 2.5 (a) and (c). Figs. 2.5 (b) and (d) shows the effect of phase difference on synchronization which is discussed in detail in Section 2.4.

2.3 Controlling chaos

Chaos occurs in many systems naturally and in many cases chaos is a nuisance. Hence control of chaos has been an important research field with a great deal of work going on. The process of controlling chaos is classified into two broad categories. The first is the feedback method where some feedback process is employed to maintain the trajectory in the desired mode. The second is the nonfeedback method where the knowledge of the system is used to modify chaotic behavior. Feedback method do not change the system and it usually stabilizes the unstable periodic orbits. On the other hand nonfeedback method slightly changes the controlled system, mainly by a small permanent shift in the control parameter and changes the system behavior from chaotic to the periodic regime.

Among the feedback methods, the Ott-Grebogi-Yorke method

[77] is extremely general and makes use of the fact that a chaotic system has infinite number of periodic solutions lying within it. Implementation of specifically adapted techniques to control the system from irregular chaotic motion to one or more of these periodic solutions is proving beneficial in many physical situations [40, 41, 78, 79]. However this method requires following the trajectory and employing a feedback control system which is highly flexible and responsive. Also even small amount of noise will cause large departures from the operating trajectory. Pyragus [80] proposed two methods to control chaos. One is to use a feedback and a periodic external forcing while the second is to use a self controlling delayed feedback. These methods being noise resistant could be easily implemented in experimental systems. However nonfeedback methods have definite advantages over the feedback methods in that in the case of nonfeedback control we do not have to follow the trajectory and there is also no need to wait until the trajectory is close to the appropriate unstable orbit. Many works have been carried out by using nonfeedback control, in various chaotic systems analytically [81, 82, 83], numerically [81, 82, 83, 84, 85] and experimentally [86, 87, 88]. Virtually all engineering and natural systems are usually subjected to an external forcing. This forcing can be planned to include a component which will help to shift to a parameter space where the system is not chaotic. Periodic perturbation applied to the system as external forcing [37, 89, 90, 91] or as a perturbation to one of the internal parameters [92] is found to suppress chaos. It is even shown that the addition of a suitable random noise can change the chaotic dynamics to a periodic one [93]. Chaotic systems can also be stabilized

by applying a small time-dependent modulation to a parameter of the system. However in practical applications, this method requires that the characteristic times of the system is not too short compared with the times of the feed back. In the case of JJ oscillators, the characteristic times of the dynamics response are of the order of few picoseconds which is too short for any electronic feedback control system. A phase difference between the applied fields was found to play an important role in suppressing chaos [94]. In the following section, we study the influence of phase difference between the applied fields on suppression of chaos and synchronization in Josephson junctions .

2.4 The effect of phase difference

The question of the influence of phase difference between the applied fields in taming chaos was first addressed by Zhilin et al. [94]. They found that in a Duffing oscillator system, by properly choosing the phase difference between the two applied sinusoidal fields, one can greatly reduce the amplitude of the control forcing to achieve effective control of chaos. As phase control can be easily achieved in experiments by phase locking techniques, this has great potential applications. Another observation is that regular appearance of chaotic and periodic motions occur which are termed as breathers when the two harmonic forces slightly deviate from resonance. A phase difference between the applied fields on two chaotically synchronized Duffing oscillator was found to destroy synchronization and bring in periodic motion [95].

In order to study the effect of phase difference of the applied sinusoidal driving fields on JJ systems, we define new variable in terms of the difference between the variables as $S_\phi = \phi_1 - \phi_2$ and $S_\psi = \psi_1 - \psi_2$. The derivatives of S_ϕ and S_ψ are taken as

$$\dot{S}_\phi = \dot{\phi}_1 - \dot{\phi}_2$$

and

$$\dot{S}_\psi = \dot{\psi}_1 - \dot{\psi}_2$$

Substituting the values of $\dot{\phi}_1, \dot{\phi}_2, \dot{\psi}_1, \dot{\psi}_2$ from Eq. (2.8) we get

$$\begin{aligned} \dot{S}_\phi &= S_\psi, \\ \dot{S}_\psi &= -\beta S_\psi - \sin \phi_1 + \sin \phi_2 - 2\alpha_s S_\psi + 2i_0 \sin\left(\Omega t + \frac{\theta}{2}\right) \sin\left(\frac{\theta}{2}\right). \end{aligned} \quad (2.10)$$

First we consider the case where no phase difference is present between the applied fields. i.e., $\theta = 0$ and in this case the term $2i_0 \sin(\Omega t + \theta/2) \sin(\theta/2)$ becomes zero. By suitably choosing the values of α_s and β , it is possible to find a region where the difference between the voltages is zero. i.e., $\psi_1 \approx \psi_2$. Now both \dot{S}_ϕ and \dot{S}_ψ go to zero or the system is synchronized. The value of α_s is chosen as 0.45 which satisfies this condition.

However, even small values of applied phase differences desynchronizes the system as can be seen from Eq.2.10. The presence of θ makes the right hand side of the equation a nonzero value and hence there is no possibility of synchronization in this case. Figs. 2.5(a) and 2.5(c) show that the system is synchronized in the absence of a phase difference. The system gets desynchronized by an applied

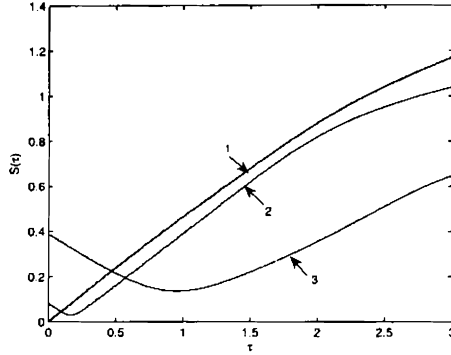


Figure 2.6: Similarity function $S(\tau)$ versus τ for different values of phase difference θ . Curve 1 is with phase difference $\theta = 0$, 2 for $\theta = 0.1\pi$ and 3 for $\theta = 0.5\pi$.

phase difference of $\theta = 0.1\pi$ as shown in Figs. 2.5(b) and 2.5(d). The level of mismatch of chaotic synchronization can be given quantitatively by taking the similarity function $S(\tau)$ as a time averaged difference between the variables ψ_1 and ψ_2 taken with time shift τ

$$S^2(\tau) = \frac{\langle [\psi_1(t + \tau) - \psi_2(t)]^2 \rangle}{[\langle \psi_1^2(t) \rangle] [\langle \psi_2^2(t) \rangle]^{1/2}}. \quad (2.11)$$

The similarity function is defined to characterize lag synchronization. This measure is similar to the cross correlation function $\langle (\psi_1(t + \tau)\psi_2(t))^2 \rangle$, but S is specially suitable to measure lag synchronization from bivariate time series because $S(\tau_0) \approx 0$ at a certain nonzero τ_0 indicates lag synchronization. So essentially we search for the minimum $\sigma = \min_{\tau} S(\tau) = S(\tau = \tau_0)$ [47]. The value $S(\tau)$ plotted against τ for different values of phase difference θ is shown in

Fig. 2.6. It is observed that for $\theta = 0$, the system is in complete synchronization. For a finite value of phase difference, a minimum of $S(\tau_0)$ appears which indicates the existence of a certain phase difference between the interacting systems. In the phase synchronization regime the curve has a clear minimum $\sigma \neq 0$. However finite $S(\tau_0)$ means that in this regime the amplitudes are uncorrelated. Thus a phase difference desynchronizes the system though for small values of phase difference, a phase correlation may be expected between the two systems.

The next aim is to check how the dynamics of the system is affected by the application of a phase difference. For this, the values of θ is varied from 0 to 2π and the value of the difference in voltage is plotted against the phase in Fig. 2.7. From the inset of Fig. 2.7, it can be seen that the system exhibits a change in the dynamics in the region where $\theta = 0.34\pi$ to 0.4π . By evaluating the time series we observe that the system exhibits periodic behavior in this region. However even a slight change in system parameter values would bring the system back to chaotic regime. For a phase difference of $\theta = 0.95\pi$ to 1.5π the system exhibits periodic motion. The difference in voltage and voltage of a single junction for $\theta = \pi$ plotted against time are shown respectively in Figs. 2.9(c) and 2.9(d). Figs. 2.9(a) and 2.9(b) show difference in voltage and voltage of a single junction against time for an applied phase difference of $\theta = 0$.

In order to explain the periodic behavior in the presence of a phase difference between the applied fields we define two new variables in the synchronization manifold. When $\phi_1 \approx \phi_2$ and $\psi_1 \approx \psi_2$ we can write $P_\phi = [\phi_1 + \phi_2]/2$ and $P_\psi = [\psi_1 + \psi_2]/2$. Taking the

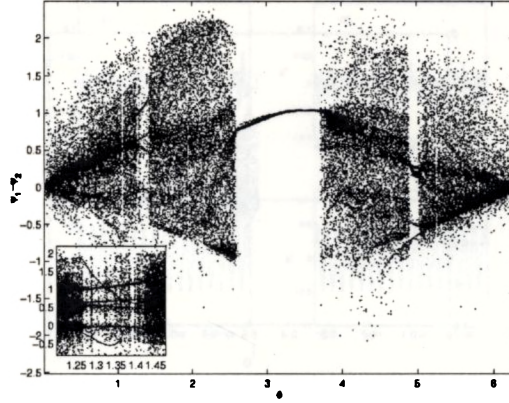


Figure 2.7: Maxima of the difference in voltage is plotted against phase difference applied, $\theta = 0 - 2\pi$. $\alpha_s = 0.45$, $i_{dc} = 0.3$, $\beta = 0.15$, $i_0 = 0.7$ and $\omega = 0.6$.

derivatives we have

$$\dot{P}_\phi = \frac{[\dot{\phi}_1 + \dot{\phi}_2]}{2}$$

and

$$\dot{P}_\psi = \frac{[\dot{\psi}_1 + \dot{\psi}_2]}{2}$$

. and from Eq. (2.8) we get

$$\dot{P}_\phi = P_\psi, \quad (2.12)$$

$$\dot{P}_\psi = -\beta P_\psi - \sin(P_\phi) + idc + i_0 \cos\left(\frac{\theta}{2}\right) \cos\left(\Omega t + \frac{\theta}{2}\right).$$

Eq. (2.12) is similar to the equation for a single Josephson junction represented by Eq. (1.13) and we can see that i_0 is replaced

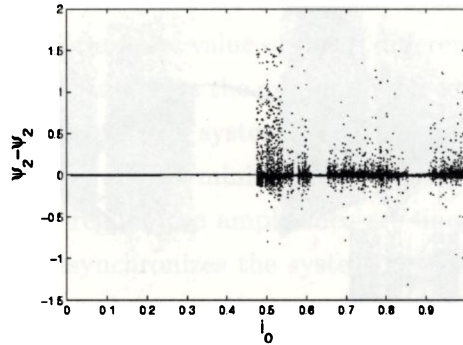


Figure 2.8: Maxima of the difference in voltage is plotted against amplitude of driving field, $\theta = 0$. $\alpha_s = 0.45$, $i_{dc} = 0.3$, $\beta = 0.15$ and $\omega = 0.6$.

by $i_0 \cos(\theta/2)$ and the phase of the driving field leads by $(\theta/2)$ as a result of coupling. The nonfeedback methods usually change the controlled system by bringing in a small permanent shift in the control parameter and change the system behavior from chaotic to the periodic regime. Thus the phase difference changed the parameter space to a region where the system is periodic. Though the effect of a phase difference seems to be similar to a change in the amplitude of the driving field, both are not equivalent. This can be seen from Fig. 2.7 and Fig. 2.8. In both cases the difference in voltage is plotted against θ and i_0 respectively and it can be seen that the system behavior is entirely different. In Fig. 2.8 the system is synchronized for values of i_0 upto 0.5 with $\theta = 0$.

From the Lyapunov exponent spectrum in Fig. 2.10 with $\theta = \pi$ it can be seen that the system is in periodic motion for most of the coupling values. The system turns from hyperchaos (two positive

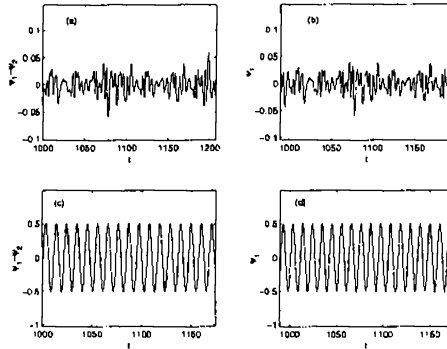


Figure 2.9: (a) shows the differential voltage plotted against time and (b) is the voltage of one junction with $\theta = 0$. It is observed that the variation is chaotic and the maximum difference in voltage is 0.05. In (c) and (d) shows the corresponding voltages with an applied phase difference of π . Other parameter values are $\alpha_s = 0.45$, $\beta = 0.15$, $i_0 = 0.7$ and $\omega = 0.6$.

Lyapunov exponent) to chaos and then to a limit cycle (two negative exponents) on increasing the coupling strength. Fixing the phase difference between the driving fields as π , the change in the response of the system to other parameter variations are then studied.

Fixing the value of α as 0.45 and the amplitude of the driving rf field is changed from 0 to 1. Without an applied phase difference the system exhibits chaotic motion from a value of 0.43 onwards with some periodic windows in between (Fig. 2.11). However, on the application of a phase difference, the system stays in periodic state for a wide range of amplitude values which are chaotic before. Fig. 2.12 shows the response of the system when the amplitude of the driving field is changed from 0 to 1 with an applied phase difference of π .

The combined effect of phase difference and the applied dc bias

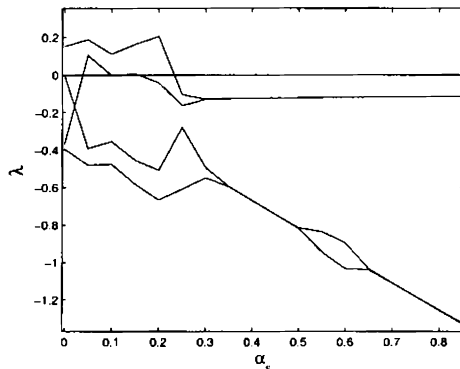


Figure 2.10: Lyapunov exponent spectrum plotted against coupling strength α_s for $\theta = \pi$, $\beta = 0.15$, $i_0 = 0.7$ and $\omega = 0.6$.

on the system is also studied. For this, all the other parameter values are fixed and i_{dc} value is changed from 0 to 0.4. First, the phase difference is taken to be zero and Fig 2.13 shows that the system exhibits chaotic behavior with some periodic windows. But for majority of values the system is in the chaotic region. However a phase difference between the applied fields changes the scenario completely. Fig. 2.14 shows that the system is periodic for most of the i_{dc} values. Thus the system exhibits periodic motion for a wide range of parameter values for an applied phase difference between the driving fields. This may be of great practical importance in JJ devices like voltage standards, SQUIDS, detectors etc.

A key point to be noted is that the parameter values at which we apply phase difference is to be chosen carefully. We are able to suppress chaos by applying a phase difference between the driving fields only in regions where the coupled systems were synchronized.

2.5 Conclusion

The role of an applied phase difference between the driving fields in a system of two coupled JJ has been studied. Suppression of chaos is found to be possible when a phase difference is applied to the system in the synchronization manifold. However, when the difference in voltage between the two junctions are not negligible, chaos cannot be controlled by just applying a phase difference between the driving fields. Though the application of a phase difference between the applied fields desynchronizes the system, a phase correlation has been found to exist for small values of applied phase differences. The difference between changing the amplitude of the driving fields and applying a phase difference between the fields has been discussed. For a phase difference of $\theta = 0.95\pi$ to 1.5π the dynamics of the system has been found to change from chaotic to periodic. By fixing the phase difference as π and varying other parameters such as dc bias, amplitude of applied field and coupling strength the change in the response of the system has been studied. It has been found that even for large variation of these parameters, the system continues to be in periodic motion. So, this may be of great practical importance as phase difference can be easily applied to the rf-field in an experimental set up. Thus, it offers an easier way to control chaos and will provide an enhanced capability to design superconducting circuits in such a way as to maximize the advantages of nonlinearity while minimizing the possibility of instabilities.

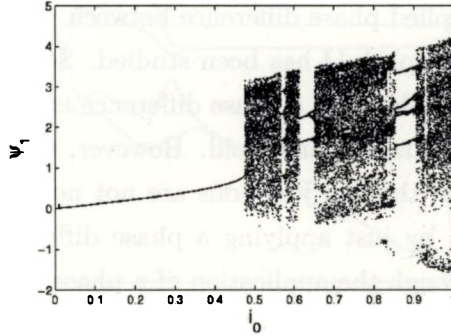


Figure 2.11: Maxima of the normalized voltage against amplitude of applied field i_0 with $\theta = 0$. The other parameter values are $\alpha_s = 0.45$, $i_{dc} = 0.3$, $\beta = 0.15$ and $\omega = 0.6$.

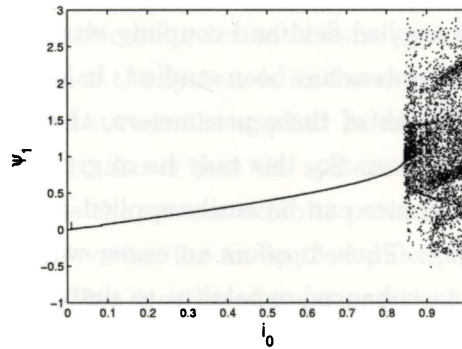


Figure 2.12: Maxima of the normalized voltage is plotted against the amplitude of applied field. It can be seen that the system is in periodic motion for a wide range of amplitude values. $\theta = \pi$, $\alpha_s = 0.45$, $i_{dc} = 0.3$, $\beta = 0.15$ and $\omega = 0.6$.

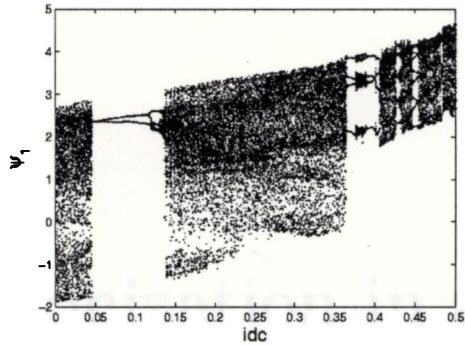


Figure 2.13: Maxima of the normalized voltage against i_{dc} . $\theta = 0$, $\alpha_s = 0.45$, $\beta = 0.15$, $i_0 = 0.7$ and $\omega = 0.6$.

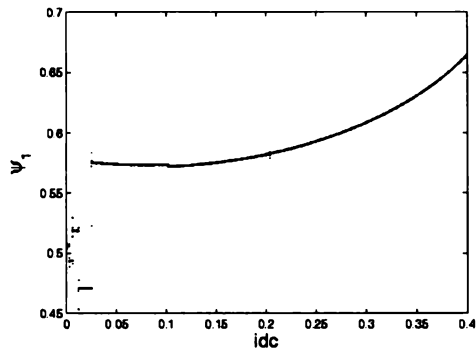


Figure 2.14: Maxima of the normalized voltage against i_{dc} . $\theta = \pi$, $\alpha_s = 0.45$, $\beta = 0.15$, $i_0 = 0.7$ and $\omega = 0.6$.

Chapter 3

Synchronization in an array of coupled Josephson junctions

3.1 Introduction

Arrays of Josephson junctions constitute one of the most intriguing examples of coupled nonlinear oscillators. The main interest in these complex systems is not just because of the richness of their physics, but also for the possibility of using these arrays in the production of cryogenic devices with unique properties and low power consumption. Josephson voltage standards [96], fast logic elements [97, 98], neural networks [99] and photofluxonic detectors [100] are some of the examples of devices made of Josephson junction arrays. The studies on Josephson junction arrays have increased during the

past few years because of the improved reliability of the lithographic and fabrication which allows a much higher degree of integration than before and the availability of inexpensive personal workstations which made simulations of discrete systems possible. Levinsen et al. conceived a new type of voltage standard from an array of Josephson junctions which promised to provide voltages much larger than that obtained from the existing voltage standards [101]. However when the experiments were performed it was observed that the current - voltage curves characterized predominantly by irregularities and noise rather than the predicted regions of constant voltage [39]. Later it was understood that these instabilities were due to deterministic chaos intrinsic to the rf-biased junction. Hence practically it is important to study chaos associated with Josephson junction arrays and methods to control it. In this chapter, we extend the studies of the influence of phase difference made in the second chapter to an array of chaotic Josephson junctions .

3.2 The model

We consider an array of Josephson junctions linked in parallel by linking resistor R_g between them. A schematic representation of an array of JJ wired in parallel with linking resistors is given in Fig. 3.1. The equation of motion for an array of N coupled current driven JJs can be written in the normalized form as

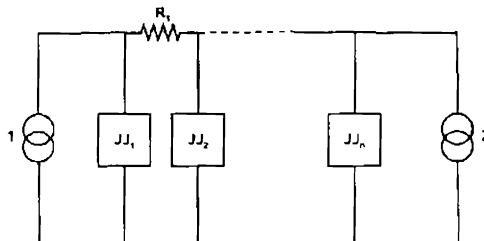


Figure 3.1: Schematic representation of an array of JJ linked in parallel with a linking resistor R_s . 1 and 2 are the driving fields.

$$\ddot{\phi}_1 + \beta \dot{\phi}_1 + \sin \phi_1 = i_{dc} + i_0 \cos(\Omega t) - \alpha_s [\dot{\phi}_1 - \dot{\phi}_2] \quad (3.1a)$$

$$\vdots$$

$$\ddot{\phi}_i + \beta \dot{\phi}_i + \sin \phi_i = \alpha_s [\dot{\phi}_{i+1} + \dot{\phi}_{i-1} - 2\dot{\phi}_i] \quad (3.1b)$$

$$\vdots$$

$$\ddot{\phi}_N + \beta \dot{\phi}_N + \sin \phi_N = i_{dc} + i_0 \cos(\Omega t) - \alpha_s [\dot{\phi}_N - \dot{\phi}_{N-1}] \quad (3.1c)$$

where i varies from 2 to $N-1$ and the dimensionless damping parameter β is defined as

$$\beta = \frac{1}{R} \sqrt{\frac{\hbar}{2ei_c}}$$

The normalized time scale is written as $t = \omega_{J1}t'$ where $\omega_{J1} = (2ei_{c1}/\hbar C_1)^{\frac{1}{2}}$. The dc bias current i'_{dc} and the rf amplitude i'_0 are normalized to the critical current i_{c1} . The actual frequency ω is re-scaled to $\Omega = \omega/\omega_{J1}$ and the coupling factor is defined as $\alpha_s = (R_1/R_s)\beta$.

These equations can be numerically simulated by using fourth order Runge-Kutta method. The Josephson junction is found to be chaotic for the parameter values $\beta = 0.3, i_0 = 1.2, \omega = 0.6$ and $i_{dc} = 0.3$. We fix these parameter values for the numerical simulations. First we take the case of three Josephson junctions and then extend it to N junctions. The junctions are taken to be identical and for a coupling strength of $\alpha_s = 0.37$, the outer junctions synchronize while the inner junction remains uncorrelated with the two outer ones. It can be seen from Fig 3.2(a) that the outer junctions are synchronized whereas Fig.3.2(b) shows that it is uncorrelated with the middle junction for an array of three JJs.

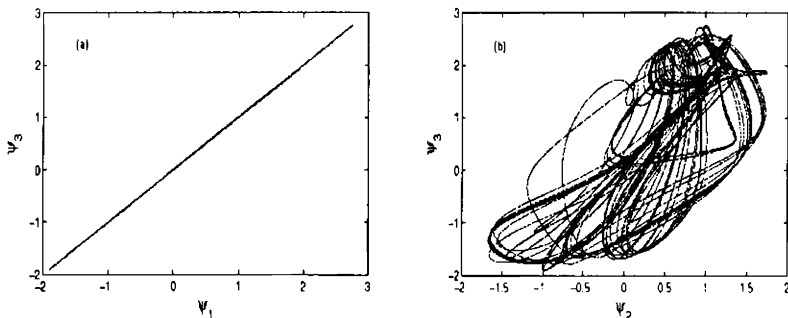


Figure 3.2: (a) The outer junctions are synchronized (b) Outer junction and middle junction is uncorrelated. The parameter values are $\beta = 0.3, i_0 = 1.2, \omega = 0.6, i_{dc} = 0.3, \alpha_s = 0.37$.

This kind of a situation where the connecting middle system remains unsynchronized with the outer systems is termed as relay synchronization. Synchronization of three laser systems are studied for relay synchronization experimentally, numerically and analytically [102]. It is observed that the outer system synchronized while the middle system remained unsynchronized with the two outer ones. The importance of this configuration lies in the similarity with the various neural models [103]. Important functional information about the brain states could be obtained by modeling it with equivalent scale-free small-world networks [104]. A configuration for such a model is given by considering three bidirectionally coupled oscillators in a line. The outer elements are seen to synchronize isochronally while the middle element lags behind. It is also verified for a neuron model with three elements that the outer elements gets synchronized while remaining lag synchronized with the middle one [105]. It is demonstrated using Rössler oscillators that during the transmission of information about a stimulus through an active array, the stimulus created the way to be transmitted by making the chaotic elements to phase synchronize [106]. The stability of synchronous state is analyzed by Lyapunov function method [107] and the master stability approach [108]

3.3 Stability analysis

In this section, we find the stability of the synchronous solution and also try to find the condition in which the middle junction might synchronize with the outer ones. In order to perform the stability

analysis for the synchronized state of N-coupled Josephson junctions, we first consider three JJs linked in parallel. In first order, Eqs. 3.1 may be represented as

$$\dot{\phi}_1 = \psi_1 \quad (3.2a)$$

$$\dot{\psi}_1 = -\beta\psi_1 - \sin \phi_1 + i_{dc} + i_0 \cos(\Omega t) - \alpha_s [\psi_1 - \psi_2]$$

$$\dot{\phi}_2 = \psi_2 \quad (3.2b)$$

$$\dot{\psi}_2 = -\beta\psi_2 - \sin \phi_2 + \alpha_s [\psi_1 + \psi_3 - 2\psi_2]$$

$$\dot{\phi}_3 = \psi_3 \quad (3.2c)$$

$$\dot{\psi}_3 = -\beta\psi_3 - \sin \phi_3 + i_{dc} + i_0 \cos(\Omega t + \theta) - \alpha_s [\psi_3 - \psi_2]$$

From Eq.3.2a and 3.2c, it can be observed that the outer junctions are identical and symmetric with interchange of variables in the absence of a phase difference θ between the applied fields. Hence there exists an identical solution for the outer systems given by $\phi_1 = \phi_3 = \phi(t)$ and this type of behavior where systems show identical behavior is called complete synchronization. The equation for the middle junction being different from the two outer ones, it may have a different solution.

The aim of the present study is to examine the behavior of the system just off the synchronization manifold. For this we define the difference variables $\phi_{13}^- = \frac{\phi_1 - \phi_3}{2}$ and $\psi_{13}^- = \frac{\psi_1 - \psi_3}{2}$ and the approximate dynamics transverse to the synchronization manifold is obtained by linearizing the corresponding subsystem consisting of the outer junctions. For this first we take the derivative of ϕ_{13}^- and ψ_{13}^- and substituting the value of ϕ_1, ϕ_2, ψ_1 and ψ_2 from eq.3.2a and

3.2c and simplifying we get

$$\begin{aligned}\dot{\phi}_{13}^- &= \psi_{13}^- \\ \dot{\psi}_{13}^- &= -\beta\psi_{13}^- - \cos\phi_{13}^+ \sin\phi_{13}^- - \alpha_s\psi_{13}^-\end{aligned}\quad (3.3)$$

Linearizing eq. 3.3 we get the approximate dynamics transverse to the synchronization manifold. In terms of the Jacobian matrix we can rewrite the above equation as

$$\begin{pmatrix} \dot{\phi}_{1,3}^- \\ \dot{\psi}_{1,3}^- \end{pmatrix} = \begin{pmatrix} 0 & 1 \\ \cos\phi_1 & -\beta - \alpha_s \end{pmatrix} \begin{pmatrix} \phi_{1,3}^- \\ \psi_{1,3}^- \end{pmatrix},$$

where $\sin\phi_{1,3}^- \approx \phi_{1,3}^-$ and $\cos\phi_{1,3}^+ \approx \cos\phi_1$ as $\phi_1 \approx \phi_3$ in the synchronization manifold. The eigen values of the matrix are

$$m_{1,2} = -\frac{(\alpha_s + \beta)}{2} \left[1 \pm \sqrt{1 + \frac{4 \cos\phi_1}{(\alpha_s + \beta)^2}} \right]. \quad (3.4)$$

The stability of the synchronous state is controlled by the eigen values $m_{1,2}$ [109, 16]. If $m_{1,2}$ are complex conjugates with negative real part, the corresponding synchronized state is stable. In the above case the average of the term in the radical is found and it is a complex number with real part greater than unity. The real part of the largest eigen value is thus found to be negative and hence satisfy the criterion for stability of synchronization.

Now we analyze the subsystem constituted by the outer and the middle junctions. We define new variables $\phi_{i2}^- = \frac{\phi_i - \phi_2}{2}$ and $\psi_{i3}^- = \frac{\psi_i - \psi_2}{2}$ where $i = 1, 3$. As the outer junctions are identical, it is

enough to study any one subsystem. So considering the case with $i = 1$, we write,

$$\begin{aligned}\dot{\phi}_{12}^- &= \psi_{12}^- \\ \dot{\psi}_{12}^- &= -\beta\psi_{12}^- - \cos\phi_{12}^+ \sin\phi_{12}^- + \frac{1}{2}[i_{dc} + i_0 \cos(\Omega t)] - \alpha_s\left(\frac{3}{2}\psi_{12}^-\right).\end{aligned}\tag{3.5}$$

From Eq. 3.5 we conclude that in the presence of an external applied field it is not possible to synchronize all the three junctions due to the asymmetry induced by the applied fields. However in the absence of an external field, an identical solution can exist for all the three junctions.

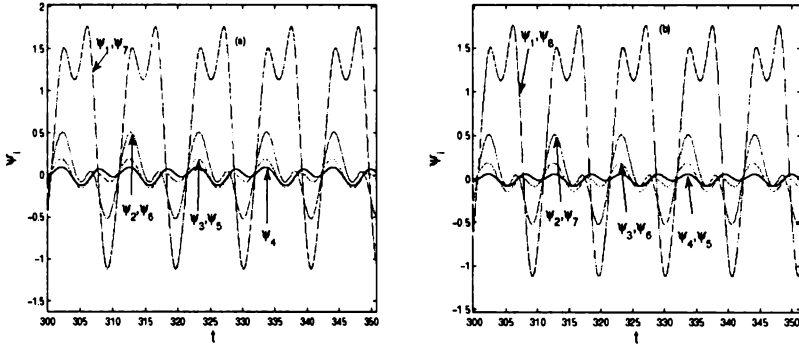


Figure 3.3: (a) shows the time series plot for an array of 7 JJs and (b) for 8 junctions. $\beta = 0.3, i_0 = 1.2, \omega = 0.6, i_{dc} = 0.3, \alpha_s = 0.37$ and $\theta = 0.5\pi$.

Extending the symmetry analysis to a system of N JJs coupled in parallel with nearest neighbor coupling, the second and the $(N - 1)^{th}$ junction may have an identical solution for certain parameter values. Similarly, the third and the $(N - 2)^{nd}$ junctions may have identical

solutions and so on. Thus in the case of an array, from symmetry considerations we may deduce that $N/2$ solutions may exist if there are even number of junctions in the array and $\frac{N+1}{2}$ solutions will be present for odd number of junctions. The time series plot for an array of 7 and 8 junctions is plotted in Fig.3.3. It can be observed from Fig.3.3(a) that in an array of seven JJs, four solutions exist for the parameter range considered. The fourth junction has an independent solution. In Fig.3.3(b) we have plotted the time series for 8 JJs.

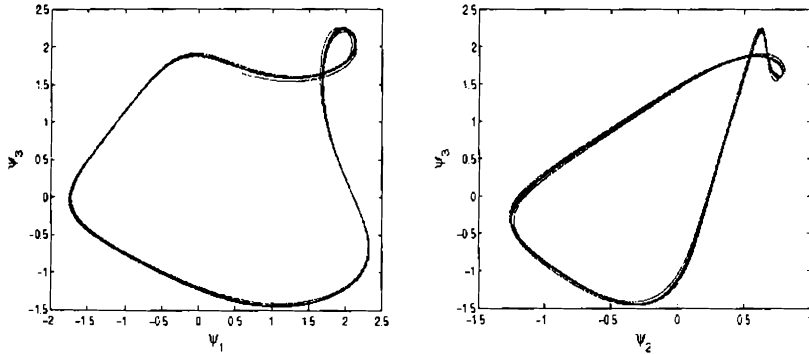


Figure 3.4: (a) and (b) shows that the junctions are phase correlated. $\beta = 0.3$, $i_0 = 1.2$, $\omega = 0.6$, $i_{dc} = 0.3$, $\alpha_s = 0.37$ and $\theta = 0.5\pi$.

3.4 Phase effect

In this section, we study the dynamics of the array in the presence of a phase difference. The presence of a phase difference between the applied fields changes the scenario completely. On the application of a small phase difference between the applied fields, the outer

junctions desynchronize and all the three junctions are thus uncorrelated. But for sufficiently large values of phase differences, all the three junctions are found to be in phase synchronization. Considering the difference variables $\psi_{1,2}, \psi_{1,3}, \psi_{3,2}$ as defined in Section 3.3, we explain the phenomena as follows. Due to the asymmetry that arises between the outer junctions in the presence of the phase difference we need the extra variable $\psi_{3,2}$ to analyze this situation. The equations for the three difference variables may be written by substituting eq.3.2 as

$$\begin{aligned} \dot{\psi}_{12}^- &= -\beta\psi_{12}^- - \cos\phi_{12}^+ \sin\phi_{12}^- + \frac{1}{2} [i_{dc} + i_0 \cos(\Omega t)] \\ &\quad -\alpha_s \left(\frac{\psi_{12}^-}{2} + \psi_{32}^- \right) \end{aligned} \quad (3.6a)$$

$$\begin{aligned} \dot{\psi}_{13}^- &= -\beta\psi_{13}^- - \cos\phi_{13}^+ \sin\phi_{13}^- + i'_0 \sin(\Omega t + \frac{\theta}{2}) \\ &\quad -\alpha_s(\psi_{13}^- - \psi_{32}^-) \end{aligned} \quad (3.6b)$$

$$\begin{aligned} \dot{\psi}_{32}^- &= -\beta\psi_{32}^- - \cos\phi_{32}^+ \sin\phi_{32}^- + \frac{1}{2} [i_{dc} + i_0 \cos(\Omega t + \theta)] \\ &\quad -\alpha_s \left(\frac{\psi_{32}^-}{2} + \psi_{12}^- \right), \end{aligned} \quad (3.6c)$$

where $i'_0 = i_0 \sin \frac{\theta}{2}$. Thus each subsystem experiences a different driving field with the same frequency but different phases. Due to the phase relationship between the driving fields, a definite phase relationship is found to exist between all three junctions as shown in Fig. 3.4.

The level of mismatch of chaotic synchronization can be given quantitatively by taking the similarity function $S(\tau)$ as a time averaged difference between the variables ψ_i taken with time shift τ

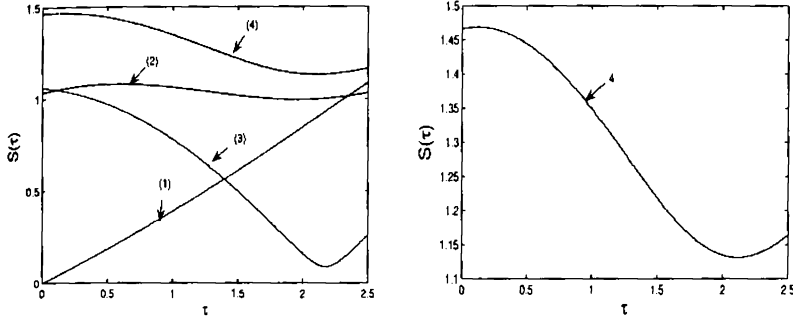


Figure 3.5: Line (1) is similarity function for variables ψ_1 & ψ_3 , (2) for ψ_1 & ψ_2 . Line (1) shows complete synchronization while the other is not synchronized. Both these lines are plotted with no phase difference applied (3) and (4) gives the similarity function for the variables ψ_1 & ψ_3 and ψ_1 & ψ_2 in the presence of phase difference $\theta = 0.5\pi$. The second figure shows line 4 where the dip can be observed clearly.

[111]

$$S^2(\tau) = \frac{\langle [\psi_1(t+\tau) - \psi_2(t)]^2 \rangle}{[\langle \psi_1^2(t) \rangle] [\langle \psi_2^2(t) \rangle]^{1/2}} \quad (3.7)$$

and

$$S^2(\tau) = \frac{\langle [\psi_1(t+\tau) - \psi_3(t)]^2 \rangle}{[\langle \psi_1^2(t) \rangle] [\langle \psi_3^2(t) \rangle]^{1/2}} \quad (3.8)$$

and searching for its minimum $\sigma = \min_{\tau} S(\tau)$. If $\psi_1(t) = \psi_3(t)$, then $S(\tau)$ has a minimum value $\sigma = 0$ for $\tau = 0$. If both $\psi_1(t)$ and $\psi_3(t)$ are independent then $S(\tau) \approx 1$ for all the time. Line 1 in Fig. 3.5 shows complete synchronization between the end junctions and line 2 shows that the outer and middle junctions are desynchronized when no phase difference is present. A minimum of $S(\tau)$ indicates the existence of a time shift between the two variables related to the

phase shift. The amplitudes are uncorrelated in this regime, but phase correlation is present as indicated by lines 3 and 4 in the presence of a phase difference between the applied fields.

On the application of a phase difference of $\pi/2$ the dynamics changes to periodic one as can be seen from Fig. 3.6

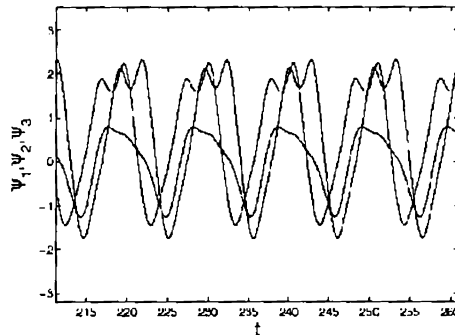


Figure 3.6: The variables corresponding to the three JJs are plotted against time which indicates the periodic behavior.

3.5 Result and discussion

We consider a parallel array of JJs with linking resistor R_s and the conditions for complete synchronization is discussed. The outer junctions being symmetric, can possess identical solution and hence may synchronize depending on the parameter values. Linear stability analysis is done to find the stability of the synchronous solution of the outer junctions. From symmetry considerations we show that all three junctions could be synchronized only in the absence of an

external field. Similarly in an array of N Josephson junctions, $N/2$ identical solutions may exist if the number of junctions is even and $\frac{N+1}{2}$ solutions may exist if the number of junction is odd. In the presence of a small phase difference, the system desynchronizes due to the asymmetry induced by the phase difference. As the phase difference is increased, in the case of three junctions all the three junctions act as if they are driven by different driving fields having the same frequency, but different phases. A phase synchronization is observed between all the three junctions and the motion becomes periodic. Thus, suppression of chaos can be obtained in Josephson junction systems in the presence of a phase difference between the applied fields and this property may find applications in the working of devices constructed using JJs.

Chapter 4

Effect of phase difference on bidirectionally coupled system with time-delay

4.1 Time-delay systems

Time-delayed systems are interesting because the dimension of chaotic dynamics can be made arbitrarily large by increasing the time-delay and hence find applications in secure communications. Time-delay is ubiquitous in physical, chemical and biological systems due to finite transmission times, switching speeds and memory effects. The equations with time-delay are important because of their potential applications to the theory of automatic regulators and servomechanisms. The value of the variables in a system with time-delay is determined by the values of the variables at some previous

moments of time. The delay equation may be given as

$$\frac{dx_i}{dt} = X_i(x_1(t + \vartheta), \dots, x_n(t + \vartheta), t) \quad (4.1)$$

with $i = 1, 2, \dots, n$. $X_i(x_1(t + \vartheta), \dots, x_n(t + \vartheta), t)$ are functionals defined for piecewise-continuous functions $x_i(\vartheta)$ of the argument ϑ , which is restricted to the interval $-h \leq \vartheta \leq 0$, where h is a positive constant. Thus to determine the derivative dx_i/dt at a given moment of time, it is necessary to know the values of the functions $x_i(t + \vartheta)$ which describe the behavior of the system at the previous time which are involved in the functional X_i . The numerical value of this functional then gives the value of the derivative at an instant t . A dynamical system is infinite dimensional if an infinite set of independent numbers are required to specify the initial conditions [112]. A time-delay system is an infinite dimensional system as the values of the variable x_i in the interval $[t, t - \tau]$ is required to calculate the value at the instant t .

Delay-coupled systems, i. e. , systems where the value of the variable at a previous time of the second system is coupled to the first has been investigated for chaos and synchronization. A time lag between the oscillators is observed in the cross correlation in delay coupled systems. This is referred to as achronal synchronization and was observed theoretically [113] and experimentally [114] in laser systems. Also, when achronal synchronization occurs, the situation will sometimes get complicated by the switching between the leader and the follower [115, 116]. Anticipatory, lag, projective and phase synchronizations have been reported in time-delayed systems [117, 118, 119].

In a drive response system, the response system sometimes anticipates the dynamics of the driver. This is known as anticipatory synchronization. This has been observed in delay coupled lasers [120, 121].

A generalized stability theory for synchronized motion of coupled oscillator systems was developed by Fujisaka and Yamada [43, 44]. However the addition of a time-delay considerably complicates stability analysis by introducing an infinite number of degrees of freedom into the system. The condition for stability of synchronization for unidirectionally coupled piece-wise linear time-delayed systems can be obtained using the Lyapunov-Krasovskii method [122, 123]. Intermittent anticipatory, intermittent lag and complete synchronization are found to exist at the same time in unidirectionally coupled nonlinear time-delayed system having two different time-delays [124]. The phenomena of synchronization of the outer lasers in a system of three lasers has been explained using the ideas of generalized synchronization [110]. Isochronal synchrony in coupled semiconductor and fiber ring laser models with mutual delay-coupling was also studied [125]. Time-delay has been studied experimentally in JJ transmission lines represented by a sequence of overdamped underbiased JJs [126]. The synchronous variation of all the bias currents causes a change in the time required for the pulses to pass through the line, and hence possible to provide a required time-delay.

Most of the chaos based communication techniques use synchronization in unidirectional drive response system. A limitation which arises in this case is that messages can be sent only in one direction. Thus for a two way transmission of signals, a bidirectional coupling

is required. In this chapter, we deal with an array of three Josephson junctions coupled in a line with a finite time-delay in coupling and study the system dynamics in the presence of an external driving field. The effect of phase difference and a small frequency mismatch between the driving fields on a chaotically synchronized system with time-delay is also discussed.

4.2 Time-delay equations

The dynamical equations for three Josephson junctions with a time-delay in coupling can be given as

$$\begin{aligned}
 \ddot{\phi}_1 + \beta\dot{\phi}_1 + \sin \phi_1 &= i_{dc} + i_0 \cos(\Omega t) - \alpha_s \left[\dot{\phi}_1 - \dot{\phi}_2(t - \tau) \right] \\
 \ddot{\phi}_2 + \beta\dot{\phi}_2 + \sin \phi_2 &= \alpha_s \left[\dot{\phi}_1(t - \tau) + \dot{\phi}_3(t - \tau) - 2\dot{\phi}_2 \right] \\
 \ddot{\phi}_3 + \beta\dot{\phi}_3 + \sin \phi_3 &= i_{dc} + i_0 \cos[(\Omega + \Delta\Omega)t + \theta] - \alpha_s \left[\dot{\phi}_3 - \dot{\phi}_2(t - \tau) \right],
 \end{aligned} \tag{4.2}$$

where τ is the time-delay applied and α_s is the coupling term which takes into account of the contribution from the delay circuit. $\Delta\Omega$ is the frequency detuning and θ is the phase difference among the applied fields. Phase synchronization has been studied in a similar system of chaotic rotators without time-delay [127]. In the present work we have considered the systems to be identical and Eq. (4.2) may be written in equivalent form as

$$\begin{aligned}
\dot{\phi}_1 &= \psi_1 \\
\dot{\psi}_1 &= -\beta\psi_1 - \sin \phi_1 + i_{dc} + i_0 \cos(\Omega t) - \alpha_s [\psi_1 - \psi_2(t - \tau)] \\
\dot{\phi}_2 &= \psi_2 \\
\dot{\psi}_2 &= -\beta\psi_2 - \sin \phi_2 + \alpha_s [\psi_1(t - \tau) + \psi_3(t - \tau) - 2\psi_2] \\
\dot{\phi}_3 &= \psi_3 \\
\dot{\psi}_3 &= -\beta\psi_3 - \sin \phi_3 + i_{dc} + i_0 \cos[(\Omega + \Delta\Omega)t + \theta] - \alpha_s [\psi_3 - \psi_2(t - \tau)].
\end{aligned} \tag{4.3}$$

For the case $\Delta\Omega = \theta = 0$, it can be seen from Eq. 4.2 that the sub-systems consisting of the outer JJs possess symmetry with respect to interchange of variables and hence may possess identical solutions. This type of situation where identical solutions exist for coupled systems is known as complete synchronization. Chaotic systems also exhibit complete synchronization for some values of parameters. An array of JJs with no delay in coupling is found to be chaotically synchronized for the parameter values $\beta = 0.3, i_0 = 1.2, \Omega = 0.6, i_{dc} = 0.3$ with $\alpha_s = 0.37$ [128]. We have selected these values of parameters for numerical studies unless specified otherwise. In the presence of a time-delay in coupling, it is found that the dynamics changes between periodic and chaotic motions. However synchronization is found to be unaffected by the time-delay.

4.3 Stability analysis

In order to check for the stability of synchronization and its dependence on various parameters, we need to know the transverse Lya-

Lyapunov exponents (TLE) and its dependence on the parameters. The necessary and sufficient condition for stability of the synchronous solution is that all the transverse Lyapunov exponents (TLE) calculated with respect to the perturbation out of the synchronization manifold should be negative. However calculation of Lyapunov exponents gets complicated when time-delays are involved. By linearizing the equation for the outer JJs about the synchronization manifold, we can arrive at a necessary condition for synchronization, i.e., the sum of the TLE should be negative. If the sum of the TLEs is negative, it implies that the phase space is shrinking. Let $\phi(t)$ and $\psi(t)$ represent the synchronous solution and we define new variables $\Delta\phi_i(t) = \phi_i(t) - \phi(t)$ and $\Delta\psi_i(t) = \psi_i(t) - \psi(t)$ with $i = 1, 3$. Here $\Delta\phi_i(t)$ and $\Delta\psi_i(t)$ are the perturbations of the outer oscillators from the synchronization manifold. Linearizing Eq.4.3 transverse to the synchronization manifold, we get after dropping the subscripts [110]

$$\begin{pmatrix} \Delta\dot{\phi} \\ \Delta\dot{\psi} \end{pmatrix} = \begin{pmatrix} 0 & 1 \\ 1 & -\beta - \alpha_s \end{pmatrix} \begin{pmatrix} \Delta\phi \\ \Delta\psi \end{pmatrix}.$$

We have approximated $\sin(\Delta\phi) \approx \Delta\phi$ as $\Delta\phi$ is small. Due to the delay in coupling, perturbations will not affect the coefficient matrix until $t - t_1 \geq 2\tau$. The Wronskian of the linearized system can be related to the trace of the matrix by Abel's formula

$$W(t) = \begin{vmatrix} \Delta\phi & \Delta\psi \\ \Delta\dot{\phi} & \Delta\dot{\psi} \end{vmatrix} = \exp\left(\int_{t_1}^t (-\alpha_s - \beta) dt\right).$$

The Wronskian gives the phase space dynamics of the system. Taking the natural log of the Wronskian we get

$$\ln[W(t)] = \ln |\Delta\phi\Delta\dot{\psi} - \Delta\psi\Delta\dot{\phi}| = - \int_{t_1}^t (\alpha_s + \beta) dt. \quad (4.4)$$

This is a monotonically decreasing function of t which means that the phase space volume of the system perturbed from the synchronization manifold contracts as a function of time. The sum of the transverse Lyapunov exponents is given as [110]

$$\sum_{j=1}^2 \lambda_j = \lim_{t \rightarrow \infty} \frac{1}{t} \ln |\Delta\phi\Delta\dot{\psi} - \Delta\psi\Delta\dot{\phi}|, \quad (4.5)$$

The sum of the transverse Lyapunov exponents can be now approximated using Eq. 4.4 as

$$\lambda_1 + \lambda_2 \approx -(\alpha_s + \beta). \quad (4.6)$$

which is negative indicating that the phase space of the coupled system shrinks to a trajectory representing the synchronous state. The sum of the Lyapunov exponents depends on the coupling term and damping parameter. Even though the sum of the conditional Lyapunov exponents is negative, if one of the exponents is positive, the solution will blow up along the unstable direction. This kind of a situation, where isochronally synchronized solution gets unstable even though the sum of Lyapunov exponents is negative was addressed in ref. [125]. The quality of synchronization is usually quantified using

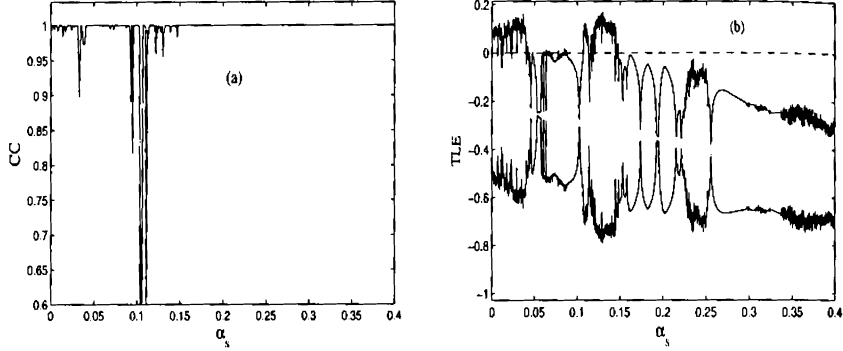


Figure 4.1: (a) Crosscorrelation (CC) between the two outer JJs for different values of coupling strength with all other values $\beta = 0.3, i_0 = 1.2, \Omega = 0.6, i_{dc} = 0.3$ (b) Transverse Lyapunov exponents plotted for the same parameter values. $\tau=0.1$ in both cases.

the correlation coefficient (CC) given by

$$CC = \frac{\langle [\psi_1(t) - \langle \psi_1(t) \rangle] [\psi_i(t) - \langle \psi_i(t) \rangle] \rangle}{\sqrt{\langle |\psi_1(t) - \langle \psi_1(t) \rangle|^2 \rangle} \sqrt{\langle |\psi_i(t) - \langle \psi_i(t) \rangle|^2 \rangle}} \quad (4.7)$$

with $i = 2, 3$. The value of correlation coefficient lies between $-1 \leq CC \leq 1$ with large value of $|CC|$ meaning better synchrony. The cross correlation of the dynamics is shown in Fig.4.1(a) for the JJ system, from which we observe that for very low values of coupling constant there is loss of synchrony. In Fig.4.1(b) the transverse Lyapunov exponents are plotted. In order to numerically evaluate TLE the difference between the variables is defined. The linearized equation corresponding to the difference equations are found out. Then the original nonlinear equation together with the nonlinear

equations are evolved numerically. A sample program is given in Appendix A.1. It can be seen that the sum of the TLE will always be negative as given by Eq.4.6. We observe that corresponding to the

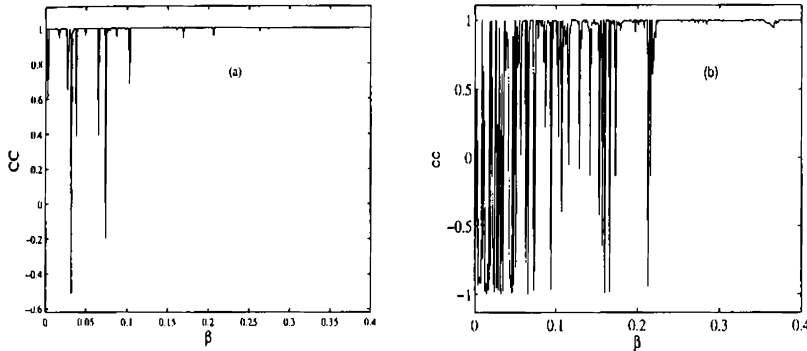


Figure 4.2: (a) CC between the two outer JJs for different values of damping parameter with $\alpha_s = 0.37$ (b) CC between the outer and middle junction.

values where cross correlation is lost, there is a small positive value for one of the TLE. Thus by comparing the cross correlation with the stability condition one can obtain a qualitative idea about the nature of the TLE. In the coupling scheme we considered as in the difference equation the time-delay part get canceled the evaluation is not so tedious. However if time-delay comes in the difference equations, then the evaluation of Lyapunov exponent is difficult as the system will have infinite dimension. In such cases this method may be used to know the nature of TLE without explicitly evaluating them. Fig.4.2 (a) shows the cross correlation between the outer junctions for various values of damping parameter. It can be observed from Fig.4.2 (b) that the middle junction remains uncorrelated with the

outer ones for most of the values of damping parameter. Thus the middle junction mediates synchronization between the outer junctions while remaining unsynchronized with both the outer junctions.

In the presence of a time-delay τ , the dynamics of the system changes considerably. It is observed that for some values of time-delay (for τ nearly equal to 0.35 onwards) the system exhibits periodic synchronized motion. Fig. 4.3(a) is the bifurcation plot for various time-delays which shows periodic and chaotic behavior for different delay times. With Fig. 4.4(a), we show that the system remains synchronized for most of the values of time-delay. The TLEs plotted in Fig. 4.4(b) show that one of the TLEs has positive value for regions where CC is lost.

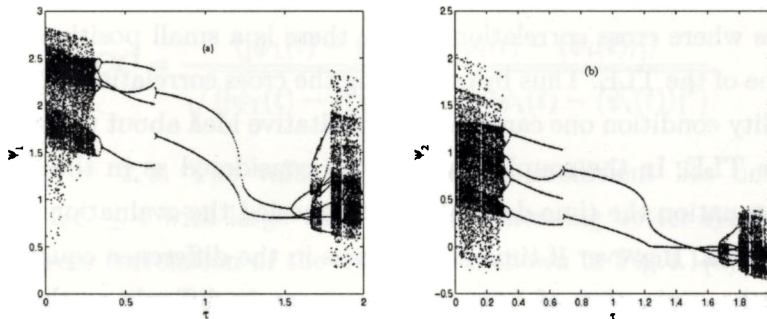


Figure 4.3: (a) Bifurcation diagram for ψ_1 against τ (b) Bifurcation diagram for ψ_2 against τ . Parameter values are $\beta = 0.3, i_0 = 1.2, \Omega = 0.6, i_{dc} = 0.3, \alpha_s = 0.37$

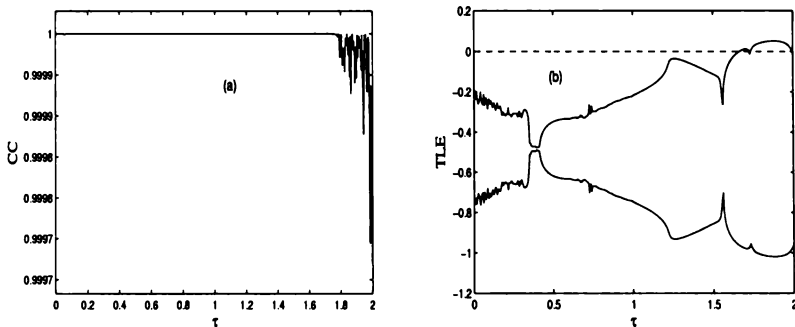


Figure 4.4: (a) Cross correlation for various values of τ with the other parameter values as $\beta = 0.3, i_0 = 1.2, \Omega = 0.6, i_{dc} = 0.3, \alpha_s = 0.37$ (b) TLEs plotted for different values of τ

4.4 Effect of phase difference and frequency detuning

A phase difference between the applied fields is found to suppress chaos effectively in an array of coupled Josephson junctions. In this section, we study the effect of phase difference in bidirectionally coupled time-delay systems. From Eq. 4.2, we can see that in the presence of an applied phase difference, the equation for the outer junctions is no longer identical. In terms of the difference variable $\psi_{1,3}^- = \psi_1 - \psi_3$ we can write the equation for the outer junctions from Eq. 4.3 as

$$\dot{\psi}_{1,3}^- = -\beta\psi_{1,3}^- - 2 \cos\left(\frac{\phi_{1,3}^+}{2}\right) \sin\left(\frac{\phi_{1,3}^-}{2}\right) + i_0' \sin(\Omega t + \theta/2) - \alpha_s \psi_{1,3}^- \quad (4.8)$$

where $\phi_{1,3}^- = \phi_1 - \phi_3$, $\phi_{1,3}^+ = \phi_1 + \phi_3$ and $i'_0 = 2i_0 \sin(\theta/2)$ and it can be seen that for a finite value of phase difference the outer junctions cannot get synchronized. The phase difference which usually desyn-

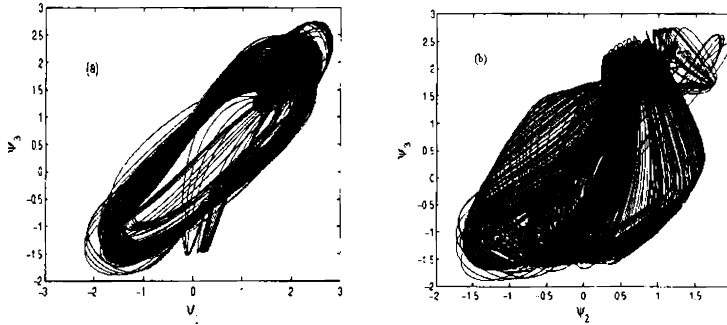


Figure 4.5: The outer and inner junctions are desynchronized on the application of a phase difference $\theta = 0.15\pi$ with $\tau = 0$.

chronizes the system may be used to suppress chaos in time-delayed systems. From Figs. 4.3 and 4.4, it can be seen that for a time-delay of $\tau = 0.25$ the system is chaotic and synchronized. Fig. 4.5 shows that an applied phase difference of $\theta = 0.15\pi$ desynchronizes the system with $\tau = 0$. But when a time-delay along with a phase difference is applied the system exhibits periodic motion. From the time series plotted in Fig. 4.6, it can be observed that the application of a phase difference $\theta = 0.15\pi$ along with the time-delay, the system goes to a periodic state. To complete the discussion, we consider the case of frequency detuning as it is difficult to apply a second frequency which is exactly same as the first. Small deviations in the applied frequencies are inevitable. So we consider the system with a small frequency detuning and the initial phase differ-

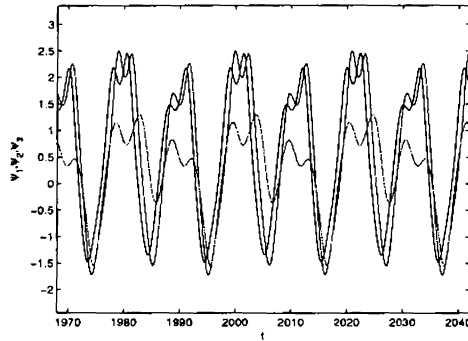


Figure 4.6: Periodic when a time-delay $\tau = 0.25$ along with a phase difference $\theta = 0.15\pi$ applied.

ence is taken to be zero. In order to investigate the difference in the dynamics brought about by frequency detuning, we first check the case where $\Delta\Omega = 0$ in Eq.4.2, i.e, the case without any detuning. Fig. 4.7 shows the temporal dynamics of the system considered with no detuning. Fig. 4.7(a) shows the time series plot for ψ_1 with no detuning. Fig. 4.7(b) shows the time series plot for the difference between the variables of the outer and the middle junction while Fig. 4.7(c) is time series plot for the outer junctions. The outer junctions are completely synchronized while remaining uncorrelated with the inner junction. When a frequency detuning is applied, it can be observed that the outer junctions gets completely synchronized in regular intervals. Fig. 4.8(a) is the time series plot for the variable for the outer junction with $\Delta\Omega = 0.004$ and it can be seen that a periodic modulation has appeared due to detuning. Here we observe that though the qualitative behavior is repeated, the trajectory of

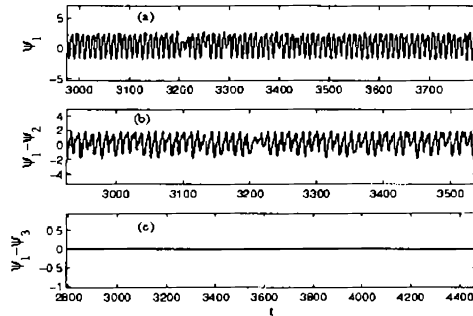


Figure 4.7: The temporal dynamics of the variable with no detuning for $\alpha = 0.37$

the system cannot be completely repeated due to the chaotic segments in the evolution process. This type of motion is referred to as breathers. Fig. 4.8(b) shows the time series plot for the difference between the variables of the outer and middle junctions and it can be seen that they remain uncorrelated. Fig. 4.8(c) shows the time series plot for the difference between the variables of the outer junctions. It can be seen that they get synchronized periodically with a period of $T = 2\pi/\Delta\Omega$. The qualitative behavior of the system is not affected by time delays.

4.5 Result and discussion

In this work we deal with bidirectionally coupled time-delayed systems and study the effect of delay and phase difference between the applied fields on synchronization. The sum of the Lyapunov exponents transverse to the synchronization manifold is evaluated and

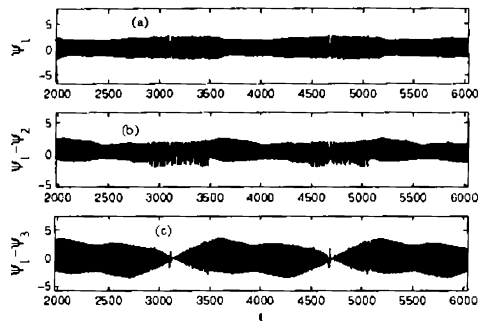


Figure 4.8: The temporal dynamics of the variable with $\Delta\Omega = 0.004$ for $\alpha = 0.37$

it is found to be negative indicating the shrinking of phase space of the coupled system to a trajectory representing the synchronous state. However cross correlation coefficient reveals positive TLE for some values of coupling constant and damping parameter where synchrony is lost, though the sum would be still negative. Transverse Lyapunov exponents are evaluated numerically and are found to be in good agreement with the analytic results. By varying the time-delay, we have analyzed the behavior of the system and it is observed that for small values of time-delays, periodic motion occur and as the delay time is increased chaotic motion reappears. However the system remained synchronized for most of the values of time-delay and hence may find applications in secure communication. The study on a configuration of three oscillators in a line is of importance because of the current recognition that it has resemblance with neuron models. Phase difference between the applied fields together with the time-delays may be effectively used to suppress chaos. The practical

situation where a small frequency detuning will be present between the applied fields is also studied. As the frequency detuning is like a time dependent phase difference, periodic and chaotic motions are repeated with a period of $T = 2\pi/\Delta\Omega$. Time-delay does not change the effect of frequency detuning. Experimentally it is possible to apply a required delay in JJ [126]. Hence by suitably adjusting the time-delay, chaos may be controlled in JJ devices like voltage standards, detectors, SQUIDS etc where chaotic instabilities are least desired.

Chapter 5

Dynamics of semiannular Josephson junctions with external ac-biasing

5.1 Introduction

A long Josephson junction serves as a very good system for studying nonlinear phenomena such as excitation of a fluxon and an anti-fluxon, their propagation, interaction, scattering and breakup. The study of fluxon dynamics is important as it is employed in the fabrication of devices like constant voltage standards [35, 129], flux flow oscillators [130, 131], logic gates [132, 133] and also in qubits [134, 135]. LJJ's of various geometries have been thoroughly studied both experimentally and theoretically in the past. The dynamical properties like fluxon pinning [136], fluxon trapping [137], and phase locked states

have been studied for rectangular [138, 139] and annular [140] LJJs.

Semiannular geometry for Josephson junction was proposed by Shaju et al. which consisted of the half an annular junction [12]. From the numerical study of the fluxon dynamics of this system, it was found to have many practical applications [141]. It has been shown that in the presence of an external magnetic field applied parallel to the dielectric barrier of such a geometry, the ends of the junction has opposite polarities. Because of this effect opposite polarity fluxons can enter the junction from the ends under a properly biased dc-current. If the direction of the current is reversed, flux penetration and progression are not possible and flux free state exists in the junction. Thus this junction behaves as a perfect diode[142]. Semiannular geometries with the magnetic field applied in the plane of the dielectric barrier was found to have application in bidirectional oscillators, current rectifiers and in rf magnetic field rectifiers[143]. The response of a fluxon to an ac-drive was investigated by several authors. It was shown that in a system with periodic boundary conditions average progressive motion of fluxon commences after the amplitude of the ac-drive exceeds a certain threshold value [144]. Complex switching distributions has been obtained for ac-driven annular JJs and theoretical explanation has been provided for the multipeaked experimental observations [145]. The behavior of fluxon under two ac forces has been studied and it was shown that the direction of motion of fluxon is dependent on the ratio of frequencies, amplitudes and phases of the harmonic forces [146]. In this chapter, we study the effect of an ac-bias applied in the plane of a semi-annular Josephson junction. This method of applying ac- biasing offers a much eas-

ier and controllable way to induce a harmonic periodic modulation to the junction. Providing modulation in the junction is important from an application point of view because of its importance in synchronizing the Josephson oscillations in a stack for the emission of electromagnetic radiation in the tetrahertz range [70]. We demonstrate creation and annihilation of fluxons in semiannular Josephson junctions in the presence of an ac-bias and an external magnetic field. The current-voltage characteristics is studied and the regime of chaos is identified.

5.2 Semiannular Josephson junction

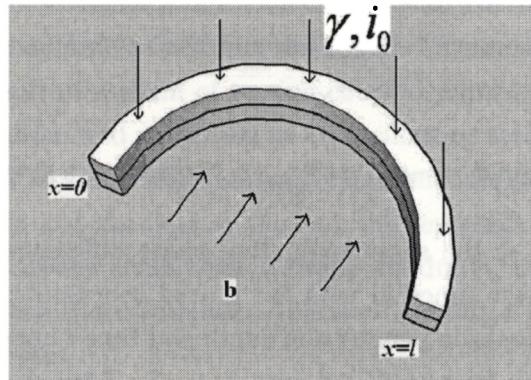


Figure 5.1: Semiannular Josephson junction with magnetic field in plane

The semiannular Josephson junction consists of half of an annular junction as shown in Fig. 5.1. In the configuration considered, the semiannular junction is under the influence of an in-plane magnetic field applied perpendicular to the plane containing the junction

boundaries. The dynamics of such a system with ac and dc-biasings is studied here. The equation for the vortex dynamics of such a system in the presence of a static magnetic field can be written as [147]

$$\varphi_{tt} - \varphi_{xx} + \sin \varphi = -\alpha \varphi_t + \beta \varphi_{xxt} - \Delta \frac{\partial}{\partial x} (\mathbf{B} \cdot \mathbf{n}) + \gamma + i_0 \sin(\omega t) \quad (5.1)$$

In the case of a linear junction where \mathbf{n} is independent of x , the presence of a homogenous magnetic field makes no perturbation inside the junction and the influence would be through the boundaries alone. However if the junction has semiannular or any other shape, there would be perturbation to the interior of the junction [11].

In the presence of a homogenous static magnetic field, the equation for a semiannular Josephson junction as obtained from Eq. 5.1 is

$$\varphi_{tt} - \varphi_{xx} + \sin \varphi = -\alpha \varphi_t + \beta \varphi_{xxt} - b \cos(kx) + \gamma + i_0 \sin(\omega t) \quad (5.2)$$

where $\varphi(x, t)$ is the superconducting phase difference between the electrodes of the junction with the spatial coordinate x normalized to λ_J , the Josephson penetration depth and time t normalized to the inverse plasma frequency ω_0^{-1} and $\omega_0 = \frac{\tilde{c}}{\lambda_J}$, \tilde{c} being the maximum velocity of the electromagnetic waves in the junction. R is the resistance per unit length, L_p is the inductance per unit length, C is the capacitance per unit length, and $\gamma = \frac{I}{j_0}$ is the normalized amplitude of a dc-bias normalized to maximum Josephson current j_0 and $i_0 \sin(\omega t)$ is the applied ac-biasing. α is the quasiparticle tunneling loss and β is the surface loss term in the electrodes and their values

vary from 0.001 to 0.3 in experiments[148]. The $\beta\varphi_{xxl}$ term gives the dissipation caused by the flow of normal electrons parallel to the barrier. The term $b \cos(kx)$ is due to the semiannular geometry of the junction and $k = \frac{\pi}{l}$ and $b = 2\pi\lambda_J\Delta Bk/\Phi_0 = 2k(B/B_{c1})$, where $B_{c1} = \frac{\Phi_0}{\pi\Delta\lambda_J}$ is the first critical field of the Josephson junction and B is the applied magnetic field. $\Phi_0 = \frac{h}{2e}$ is the flux quantum and its value is $2.064 \times 10^{-15} Wb$. The extra term $b \cos(kx)$ corresponds to a force that drives fluxons towards the left and anti fluxon towards the right. Thus in the absence of an external field a flux free state will exist in the junction as any static trapped fluxon present in the junction will be removed [141]. In this configuration the external magnetic field link only with the interior of the junction and not with the boundaries [141]. The boundary conditions of the junction are $\phi_x(0, t) = \phi_x(l, t) = 0$. It may be helpful to view Eq. 5.2 to the continuum limit of a chain of torsion coupled pendula immersed in a viscous medium and subjected to an oscillatory torque [149] with γ and b equal to zero. The term ϕ_{xx} represents the interaction between pendula and the field at the end will represent the torque at the extremes of the chain. For a single pendulum $\phi_{xx} = 0$ which is similar to the short Josephson junction equations studied in the previous chapters.

From Eq. 5.2 we observe that the parameters α, β, b, γ and $i_0 \sin(\omega t)$ governs the dynamic behavior of the long Josephson junction. All these parameters influence the chaotic and periodic motion of the junction. Besides these parameters which explicitly influence the dynamics of the long Josephson junction, there are two implicit parameters which also influence the dynamics of the fluxon: the

length of the junction and the initial conditions. In the case of zero magnetic field applied, depending on the initial conditions the behavior of the perturbed sine-Gordon is different as the number of fluxons moving in a long Josephson junction is fully determined by the initial condition. However, the presence of the magnetic field and the ac-biasing applied can generate fluxons from one end of the junction.

In the absence of any perturbation Eq. (5.2) reduces to simple sine-Gordon equation with fluxon solution given by

$$\varphi(x, t) = 4 \tan^{-1} \left[\exp \frac{\sigma(x - X)}{\sqrt{1 - u^2}} \right] \quad (5.3)$$

where u is the velocity of the fluxon and $X = ut + x_0$ is the instantaneous location of the fluxon. $\sigma = \pm 1$ is the polarity of the flux quantum (which means there are two orientations for the fluxon). A quantum of flux in one direction is called the kink solution (fluxon) and that in other direction is called antikink solution (antifluxon). The perturbational parameters α and β cause both the fluxons and antifluxons to slow down, while γ term drives fluxons in one direction and antifluxon in the opposite direction. Strong perturbations, both internal and external will alter the speed and locations of the fluxons and may also create and destroy fluxons. It is necessary to establish control over such interactions for making the junctions suitable for applications as in logic gates etc.

5.3 Perturbational analysis

The presence of an external bias current gives rise to a force on the fluxon which results in the propagation of the fluxon through the junction. The effect of dissipation, damping and driving force balance among themselves leading to a steady state velocity for the fluxon. The general perturbation method developed by Rubinstein [150] was applied for the case of Josephson junction by McLaughlin and Scott [138]. In this method the effect of perturbation is assumed to influence only the dynamics of the center of mass coordinate of the fluxon and not its shape. Using perturbational analysis, the rate of change of velocity of the fluxon in an applied field may be derived in the following way. The Hamiltonian of the system is written as a combination of the Hamiltonian of the unperturbed sine-Gordon part plus the Hamiltonian of the perturbation part [138]. Energy of the unperturbed sine-Gordon system is

$$H^{SG} = \int_{-\infty}^{\infty} \left[\frac{1}{2} (\varphi_t^2 + \varphi_x^2 + 1 - \cos\varphi) \right] dx \quad (5.4)$$

Substituting(5.3) in (5.4) we get

$$\frac{d}{dt}H^{SG} = 8u(1 - u^2)^{-3/2}\frac{du}{dt}. \quad (5.5)$$

If ϕ is any solution of Eq. 5.2, we can compute

$$\begin{aligned} \frac{d}{dt}(H^{SG}) &= [\varphi_x \varphi_t]_{-\infty}^{\infty} - \\ &\int_{-\infty}^{\infty} (\alpha \varphi_t^2 + \beta \varphi_{xt}^2 + [b \cos(kx) + \gamma + i_0 \sin(\omega t)] \varphi_t) dx. \end{aligned} \quad (5.6)$$

Here the first term on the right hand side accounts for the boundary conditions and vanishes. Substituting (5.3) in above equation we obtain the equation for rate of dissipation as

$$\begin{aligned} \frac{d}{dt}(H^{SG}) &= 2\pi u (\gamma + i_0 \sin(\omega t)) - \frac{8\alpha u^2}{\sqrt{1 - u^2}} \\ &- \frac{8\beta u^2}{3(1 - u^2)^{3/2}} - 2\pi b u \sec h\left(\frac{\pi^2 \sqrt{1 - u^2}}{2l}\right) \cos(kX). \end{aligned} \quad (5.7)$$

Equating Eqs. 5.5 and 5.7 yield an expression for the rate of change of velocity

$$\begin{aligned} \frac{du}{dt} &= \frac{\pi}{4} (\gamma + i_0 \sin(\omega t)) (1 - u^2)^{3/2} - \alpha u (1 - u^2) \\ &- \frac{1}{3}\beta u - \frac{\pi}{4} b (1 - u^2)^{3/2} \sec h\left(\frac{\pi^2 \sqrt{1 - u^2}}{2l}\right) \cos(kX). \end{aligned} \quad (5.8)$$

Eq. 5.8 describes the effect of perturbations on the vortex velocity. The first term represents the effect of applied biasing, the second and the third terms represent dissipation and fourth term is due to the

effect of the external magnetic field on the semiannular geometry.

5.3.1 Expression for potential function

In this section, we obtain the expression for the potential function in the presence of an applied ac-biasing. The Lagrangian density of Eq. 5.2 with $\gamma = \alpha = i_0 = \beta = 0$ is

$$\mathbf{L} = \frac{1}{2}\varphi_t^2 - \frac{1}{2}\left(\varphi_x - \frac{b}{k}\sin(kx)\right)^2 - 1 + \cos\varphi \quad (5.9)$$

where the first term is the kinetic energy associated with the energy density of the electric field, the second term accounts for the potential energy density associated with the magnetic field and the third term represents the Josephson coupling energy density. From the potential energy density term, the change in potential energy due to the combined effect of fluxon motion and the applied field can be determined by integrating the term $-\frac{b}{k}\sin(kx)\varphi_x$ over the length of the junction [141]. The fluxon induced potential as a function of the fluxon coordinate X may be calculated as

$$U(X) = -\frac{b}{k} \int_{-\infty}^{\infty} \sin(kx)\varphi_x dx. \quad (5.10)$$

The integration over $-\infty$ to ∞ may be justified as the length of the junction is very large as compared to the size of the fluxon. Substituting Eq. 5.3 in Eq. 5.10 and integrating we get the expression for potential as

$$U(X) = -2bl \operatorname{sech} \left(\frac{\pi^2}{2l} \sqrt{1-u^2} \right) \sin(kX). \quad (5.11)$$

For $u \simeq 0$ we can write

$$U(X) = -2bl \operatorname{sech} \left(\frac{\pi^2}{2l} \right) \sin(kX), \quad (5.12)$$

which has a potential well form with the depth of the well depending on b and l . The vortex will be pinned to the potential minima as long as the bias current is smaller than the depinning current. The pinned state of a vortex corresponds to a zero voltage state. The dc-bias at which the zero voltage switches to a finite voltage is called the depinning current.

Now we arrive at an expression for the potential function of the perturbed system. In perturbational analysis, a vortex is considered as a non-relativistic particle of rest mass $m_0 = 8$ moving in one dimension. Therefore the effective potential can be obtained using the force relation

$$\frac{\partial U_{eff}}{\partial X} = -m_0 \frac{du}{dt}. \quad (5.13)$$

Substituting Eq. 5.8 in Eq. 5.13 and integration yields an expression for effective potential at $u = 0$ in the form

$$U_{eff}(X_0) = -2bl \operatorname{sech} \left(\frac{\pi^2}{2l} \right) \sin(kX_0) - 2\pi(\gamma + i_0 \sin(\omega t))X_0 \quad (5.14)$$

The potential energy function $U_{eff}(X)$ has a well form in the absence of external biasing and the fluxon will remain pinned to the center of the junction under such a potential. As the biasing is increased the potential gets tilted finally favoring the motion of the vortex. The dc-bias at which the zero voltage switches to a finite voltage is called the depinning current. Fig. 5.2 shows the form of

T405



5.3 Perturbational analysis

the potential for $b = 0.1$ for a junction of length $l = 15$ for different external biasing. It can be seen that in the presence of an external bias the potential gets tilted favoring motion of the fluxon. While moving through such a potential, the fluxon(antifluxon) after bouncing from the edge turns into an antifluxon (fluxon) and hence will move in the opposite direction. In the presence of an ac-bias, the

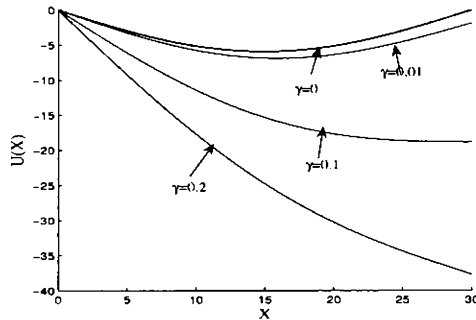


Figure 5.2: Potential well form for a JJ of length $l=15$. Other parameter values are $b = 0.1$, $i_0 = 0$. The γ value is increasing from top to bottom line.

potential gets oscillating with a frequency equal to the frequency of the applied field and the shape of the potential depends on the amplitude of the applied ac and dc-biasings. In the presence of external ac-biasing along with the dc-bias, the potential gets time varying as shown in Fig.5.3. In Fig. 5.3(a), the applied ac-bias has an amplitude of 0.1 and it can be seen that as time goes on, the potential gets a well form in a time period equal to the period of oscillation of the applied field. The applied dc-bias is 0.1 in this case. Hence progressive motion of fluxon does not occur for this value of biasing as the average velocity of a fluxon moving in such a potential would

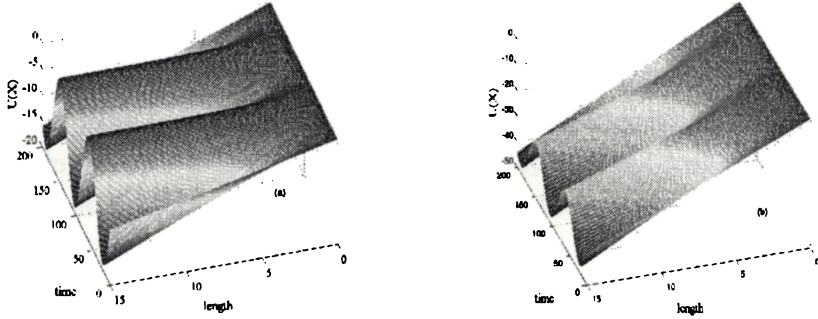


Figure 5.3: Form of the oscillating potential for a JJ of length $l=15$. Parameter values are $b = 0.1, i_0 = 0.2, \omega = 0.3, \gamma = 0.1$. a) applied dc-bias is $\gamma = 0.1$ b) $\gamma = 0.4$

be zero. However as the dc-biasing is increased though the form of the potential is still oscillating, there is a definite tilt which makes progressive motion of fluxon possible. Thus, when an ac-biasing is applied to the semi-annular JJs, progressive motion occurs only when dc-biasing value exceeds a certain threshold value which would be greater than the depinning current value in the absence of an ac-biasing. The response of the system to such a potential can be investigated by measuring the velocity of the fluxon in the potential.

5.3.2 Numerical methods

Eq. 5.2 along with the boundary conditions are studied numerically by finite difference method by representing the phase $\phi(x, t)$ by a square mesh $\phi_i^n = \phi(ih, nk)$ where h is the space step size and k is the time step size. An explicit method is used and by treating ϕ_{xx} with a five point, ϕ_{tt} with a three point and ϕ_t with a two point

finite difference method. Expressing the derivatives in the following difference form

$$\phi_t = \frac{1}{2k}(\phi_i^{n+1} - \phi_i^{n-1})$$

$$\phi_x = \frac{1}{2h}(\phi_{i+1}^n - \phi_{i-1}^n)$$

$$\phi_{tt} = \frac{1}{k^2}(\phi_i^{n+1} - 2\phi_i^n + \phi_i^{n-1})$$

$$\phi_{xx} = \frac{1}{2h^2}(\phi_{i+1}^{n+1} - 2\phi_i^{n+1} + \phi_{i-1}^{n+1} + \phi_{i+1}^{n-1} - 2\phi_i^{n-1} + \phi_{i-1}^{n-1})$$

$$\phi_{xxt} = \frac{1}{2kh^2}(\phi_{i+1}^{n+1} - 2\phi_i^{n+1} + \phi_{i-1}^{n+1} - \phi_{i+1}^{n-1} + 2\phi_i^{n-1} - \phi_{i-1}^{n-1})$$

, and substituting these in Eq.5.2, we get

$$\begin{aligned} c_1\phi_{i+1}^{n+1} + c_2\phi_i^{n+1} + c_1\phi_{i-1}^{n+1} &= c_3(\phi_{i+1}^{n-1} + \phi_{i-1}^{n-1}) - c_4\phi_i^{n-1} + c_5\phi_i^n \\ &+ c_6(\sin(\phi_i^n) + \gamma + i_{ac} \sin(\omega t) - b \cos(kx)), \end{aligned}$$

where $c_1 = \beta + k$, $c_2 = -(\alpha h^2 + (2h^2)/k + 2\beta + 2k)$, $c_3 = \beta - k$,
 $c_4 = (\alpha h^2 - (2h^2)/k + 2\beta - 2k)$, $c_5 = -(4h^2)/k$, $c_6 = 2kh^2$.

$$i = 1, 2, 3, \dots, N, \quad n = 0, 1, 2, \dots$$

The boundary conditions are treated by the introduction of imaginary points and the corresponding finite difference equation is solved using standard tridiagonal algorithm[151]. Numerical simulations are carried out on the JJ of normalized length ($l=15$). The time step is taken as 0.0125 and the space step is 0.025. The numerical results are checked by systematically halving and doubling the time steps and space steps[139, 12]. After the simulation of the phase dynamics

for a transient time, we calculate the average voltage V for a time interval T to be

$$V = \frac{1}{T} \int_0^T \varphi_t dt = \frac{\varphi(T) - \varphi(0)}{T} \quad (5.15)$$

Also for the faster convergence of the averaging procedure, the phases $\varphi(x)$ in the equation were averaged over the length of the junction. The spatial averaging increases the accuracy in the calculation of the voltages in cases where the time period over which integration is made is not an exact multiple of the time period of oscillation. Once the voltage averaging for a current γ is complete, it is increased in small steps of 0.01 to calculate the next point of the characteristic graph. The average velocity of the fluxons can be calculated from the average voltage using the relation $u = V(l/2\pi)$.

5.4 Creation and annihilation of fluxons

The dynamical properties of magnetic flux quanta are critical for the fabrication of logic devices. The motion of a fluxon is drastically modified by the presence of perturbations. The threshold for the generation of fluxon by current pulse is evaluated by Sakai et.al [152] An annular LJJ preserves the number of trapped fluxons in it. However in an open ended geometry, the number of fluxons is not a conserved quantity. In this section we investigate the creation and annihilation of fluxons in semiannular JJ with open boundary conditions in the presence of an external magnetic field together with ac and dc biasings. Three cases are considered where the initial number

of fluxons are varied. The creation or annihilation of fluxons results in a change in the voltage across the junction. Hence this investigation is of importance while designing devices as we can choose the range which is most optimal for our need.

Fluxon-fluxon interaction: The destructive line and the non-destructive line was used by Nakajima et al. [98] in the design of Josephson junction based computers. In the destructive line the fluxon and the antifluxon will annihilate on collision while in the nondestructive line they will pass through each other after collision. When a junction terminates, in a similar way, there can either be reflective or reflectionless cases depending on whether the incident fluxon disappears or gets reflected as an antifluxon. Since the boundary condition at the termination ($\phi_x = 0$) can be satisfied by assuming collision with a virtual antifluxon, the reflective and reflectionless cases are similar to the first two cases.

5.4.1 One fluxon solution

The collision of fluxons with localized obstacles leads to creation and annihilation of fluxons. The fluxon creation and annihilation process for a single fluxon solution as input is described here. A fluxon solution is launched from the center of the junction with an initial velocity of $v = 0.6$. For each value of biasing the fluxon is allowed to propagate for some time in order to stabilize its motion in the junction. The fluxon gets reflected from the boundaries and moves on till $\gamma = 0.57$. For an external magnetic field of strength 0.1 it is numerically observed that fluxon motion is not possible for a γ value higher than 0.57.

However, the presence of an ac-bias, creation and annihilation of fluxon is observed for values of dc-biasing which give one fluxon solution earlier. For a γ value of 0.1 the fluxon propagates through

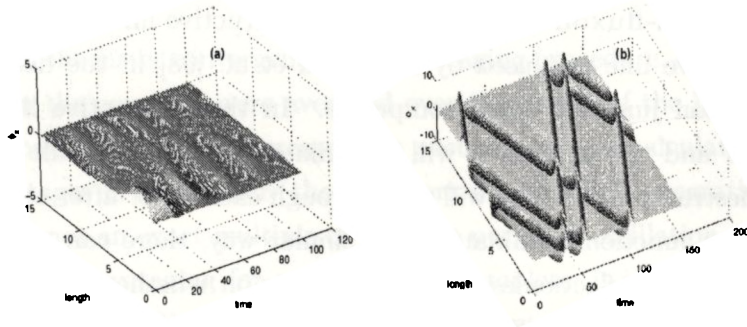


Figure 5.4: (a) The pattern shows annihilation of fluxon propagating in a JJ with $l=15$ for a dc-bias of $\gamma = 0.1$ and $i_{ac} = 0.2$. (b) Creation of fluxon with $\gamma = 0.1$ and $i_{ac} = 0.1$. Other parameter values are $\omega = 0.3$, $\beta = 0.02$, $\alpha = 0.05$, $b = 0.1$

the semiannular junction, while an ac-bias of 0.2 destroys the fluxon as can be seen from Fig. 5.4(a). Similarly Fig. 5.4(b) shows that a fluxon is created for $\gamma = 0.5$ and $i_0 = 0.1$.

5.4.2 Two fluxon solution

Two fluxon solutions are launched with at different initial points in the junction with initial velocity $v = 0.6$. An dc-biasing of more than 0.1 is needed to support motion of two fluxons in the junction. For $\gamma = 0.1$ it is observed that only a single fluxon propagates through the junction as can be seen from Fig. 5.5(a). A dc-bias of 0.12–0.45 supports two fluxon propagation in the junction in the absence of an ac-biasing. However, if an ac-bias of 0.1 is applied along with

$\gamma = 0.41$, creation of a fluxon occurs as shown in Fig. 5.5 (b).

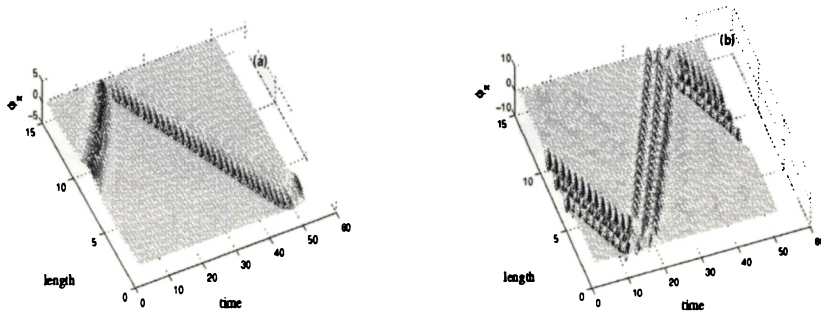


Figure 5.5: The pattern shows single fluxon propagating in a JJ with $l=15$ for $\gamma = 0.1$ for 2 fluxon input.(b)Creation of a third fluxon. $i_0 = 0.1$, $\gamma = 0.41$

5.4.3 Three fluxon solution

In this case, three fluxons are launched at different initial points. A dc-bias of $\gamma = 0.4$ is needed to support the three fluxon propagation in the junction. In Fig.5.6(a) we numerically show that only two fluxons propagate through the junction for a γ value of 0.3. Also for $\gamma = 0.4$, if an ac-bias is applied annihilation of one fluxon occurs again giving the two fluxonic propagation as shown in 5.6(a). The ac-biasing causes annihilation and if the i_0 value is increased to 0.19 or more the fluxonic profile is lost.

Creation of fluxon is observed for γ values of 0.55 as shown in Fig. 5.6(b) with ac-biasing destroying the structure even for $i_0 = 0.1$. It is to be noted that all these effects take place only in the presence of an external magnetic field in semiannular JJs. In the absence of

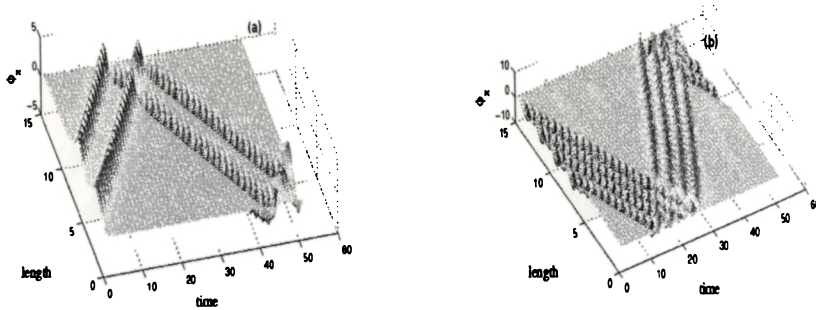


Figure 5.6: The pattern shows two fluxons propagating in a JJ with $l=15$. Other parameter values are $\gamma = 0.3$ (b)Creation of fourth fluxon $\gamma = 0.55$

magnetic fields, we are not able to observe creation and annihilation of fluxons.

5.5 Chaos in semiannular Josephson junction

Systems modeled by driven damped sine-Gordon equation have been shown to be fruitful for studying temporal chaos and spatio-temporal patterns. Since long Josephson junctions are fairly well understood, the studies on these systems will help in the understanding of the origin of chaotic dynamics in these systems. The problem of *controlling* spatiotemporal chaotic pattern induced by an applied rf signal in a JJ has earlier been discussed [153]. In this section, we study the dynamics of a semiannular Josephson junction in the presence of an external ac-biasing. As explained earlier, depending on the values of $i_0 \cos(\omega t)$, γ , β , α and b , the system may exhibit chaotic behavior. For this we first study the I-V characteristics of the system. In this

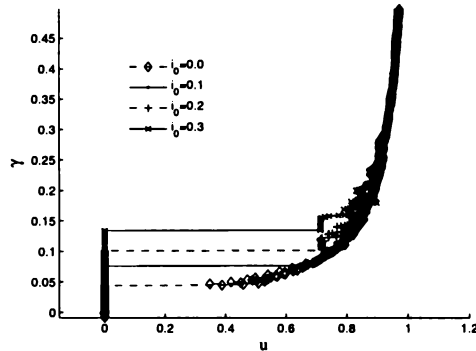


Figure 5.7: The velocity-bias characteristics of a LJJ of length $l=15$ with no external magnetic field applied. Other parameter values are $\omega = 0.3, \beta = 0.02, \alpha = 0.05$

context we neglect the surface loss term β and study the velocity change with increase in dc-biasing is observed. Fig.5.7 shows the velocity change with dc-biasing for different values of amplitude of the ac-biasing. In the presence of ac-biasing the averaging interval T is taken as a multiple of the ac drive's period $2\pi/\omega$ [144]. If an ac-biasing is present, the depinning current is found to increase which can be seen from Fig.5.7.

In the presence of external magnetic fields, the velocity versus dc-bias is shown in Fig. 5.8. The value of dc-bias to cause a finite velocity for the fluxon in a JJ with a magnetic field of $b = 0.1$ and no ac-biasing is 0.1 while for $b = 0$ the depinning current is 0.04. Thus the external magnetic field also increases the depinning current value. The depinning current to be applied to the semi-annular JJ in the absence of ac-bias, and a magnetic field of $b = 0.1$ is 0.125.

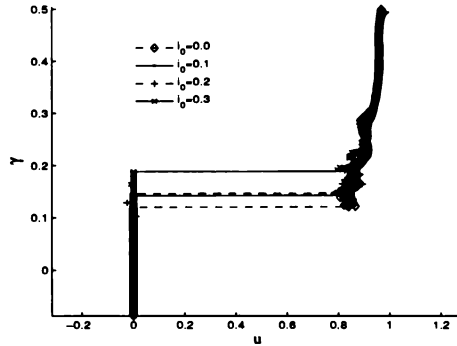


Figure 5.8: The velocity- bias characteristics of a LJJ of length $l=15$ in the presence of an external magnetic field $b = 0.1$.

Also for an ac-bias of amplitude 0.2 and 0.3 the velocity shoots to a higher value even for a dc-biasing of 0.46 and 0.36 as shown in Fig. 5.9. Quasiperiodic or chaotic motion may exist in the system for higher values. In order to identify if ac-biasing makes the system chaotic, we follow the averaging procedure given by Goldobin et al. [144]. For finding the voltage given in Eq. 5.15, the averaging is done over one period $2\pi/\omega$ of the ac drive and the amplitude i_0 is changed in extremely small steps, say $\delta i_0 = 0.0001$. Thus we get very closely situated points and if the dynamics is chaotic all these points will have a large spread in the value of average velocity and hence voltage. On the other hand if the dynamics is regular all the values will have almost same value. Though some artifacts may appear in the regimes of bifurcation, this method has proved good enough to get an insight into the dynamics of the system. Fig. 5.10 shows the bifurcation plot for a semiannular junction in the presence of an

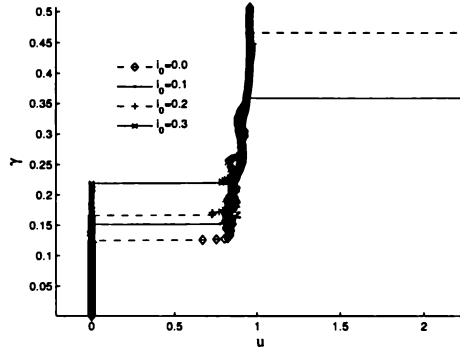


Figure 5.9: The velocity- bias characteristics of a LJJ of length $l=15$ in the presence of an external magnetic field $b = 0.1$. The damping parameter $\beta = 0.035$

ac-biasing. A sample program is given in Appendix A.2.

5.6 Conclusions

We have studied the dynamics of a fluxon trapped in a semiannular JJ in the presence of an external magnetic field along with an ac-biasing. This method of applying ac-biasing offers a much easier and controllable way to induce a harmonic periodic modulation to the junction. In the presence of an external magnetic field the vortex remains pinned in the potential well. The ac-biasing modulates the form of the potential and we obtain an oscillating potential with frequency of oscillation equal to the driving field. The change in the pinning current brought about by the ac field may be used for detection of such fields. In the presence of an ac-drive and magnetic

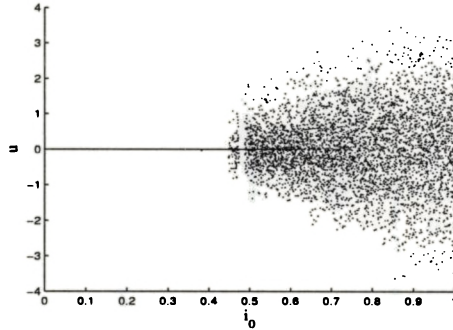


Figure 5.10: The average velocity versus i_0 plotted by increasing the value by $\delta i_0 = 0.0001$. The scattered points corresponds to the regions of chaotic motion.

field, fluxon creation and annihilation phenomena are observed. This has been demonstrated for one, two and three fluxons and can be extended to higher number fluxons. Higher values of ac-amplitudes induces chaotic dynamics in the junction. The fluxon creation and annihilation process being crucial for the understanding of the internal dynamics of the junctions, it will have important applications in the design and fabrication of superconducting digital devices.

Chapter 6

Results and discussion

Josephson junction has been proved to be an ideal candidate for the study of nonlinear dynamics and chaos. In this thesis, we study the response of the Josephson junction system to an applied ac bias. The main conclusion of the thesis are as follows.

1. A phase difference between the applied fields in a bidirectionally coupled Josephson junction system desynchronizes the synchronized system, while certain values of phase difference brings the system from chaotic to periodic regime. The system remained in the periodic regime for large changes in the control parameter values in the presence of an applied phase difference.
2. In the case of a system with three Josephson junctions connected parallelly, relay-synchronization is observed, i. e., the outer junctions got synchronized while remaining uncorrelated with the middle junction. A phase correlation exists between

all the three junctions in the presence of a phase difference between the applied field. In an array of N Josephson junctions we find that $N/2$ identical solutions can exist if the number of junctions is even and $\frac{N+1}{2}$ solutions can exist if the number of junction is odd.

3. Transverse Lyapunov exponents evaluated for delay coupled Josephson junctions reveals that the system can remain synchronized for most of the values of time-delay. Time-delay along with a phase difference between the applied fields is found to suppress chaos. Thus a phase difference between the applied fields proves to be an efficient non feedback method to control chaos as a phase difference can easily be provided in an experimental set-up.
4. In the presence of an ac-biasing, the fluxon in a long Josephson junction experiences an oscillating potential which increases the depinning current. Creation and annihilation of fluxons occur in the presence of an ac biasing together with the magnetic field. Chaotic behavior is observed for high amplitudes of ac-biasing.

Future prospects

A square network of short Josephson junctions need to be investigated for the effect of phase difference between the applied fields and also to find how the oscillators influence each other because this study can help in the development of neural networks. This

should be done for the time-delayed case also which is of importance in secure communication. Chaotic phase synchronization and the effect of phase difference between the applied fields on phase synchronization need to be investigated as this can reveal important dynamical behavior of the system.

Long Josephson junctions need to be coupled and the effect of phase difference between the applied fields on the system need to be studied in order to find whether suppression of chaos can be achieved by applying a phase difference in this case.

Appendix A

Numerical Programs

A.1 Transverse Lyapunov Exponent

Program for finding transverse Lyapunov exponents.

```
      program josephson
c   Code for Lyapunov exponent by Wolf et.al. modified for
c   transverse Lyapunov exponent of the time-delay system.
c   The nonlinear equations are numerically integrated using
c   fourth order Runge-Kutta method.
c   n = number of nonlinear odes
c   nn =n*(n+1)= total number of odes
c   nn1=nn+1 (for compilers that start arrays at element 0)
c
      implicit none
      integer n,nn,nn1,i,j,m,nstep,irate,io,k,l,it
      integer mm,q, o,oo
      parameter (n=7, nn=11, nn1=12, q=10)
      double precision y(nn),yprime(nn),v(nn),A(nn),B(nn),C(nn)
      double precision ll(q),dd(q),ee(q)
```

```

double precision D(nn),cum(2),znorm(2),gsc(2)
double precision t,tme,stpsze,cou,be,omega,idc,iac,ic,delc
external fcn
open(unit=1,file="input")
open(unit=2,file="delay.dat")
c open(unit=3,file="var.dat")
c NSTEP is the total number of reorthonormalization steps that
c will be performed.
c IRATE is the number of numerical integration time steps per
c reorthonormalization.
c STPSZE is the integration stepsize in seconds.
c IO is the rate at which output is generated.
c
write(*,111)
111 format(1x,'nstep, stpsze, irate, io : ')
read(1,*) nstep,stpsze,irate,io
c
c initial conditions for nonlinear ODEs
c (** Choose within the system's basin of attraction **)
c
delc = 0.001d0
ic = 0.0d0
do 1000 it=1,1000
cou=ic+delc*real(it-1)
be = 0.3d0
omega= 0.6d0
idc = 0.3d0
iac = 1.2d0
write(*,*)'beta,cou,alpha=',be,cou,idc
v(1:7) = 0.1356
ll(1:10) = 0.0
dd(1:10) = 0.0
ee(1:10) = 0.0

```



```

      tme = 0.0
      cum(1:2) = 0.0

c
c   initial conditions for linearized ODEs
c
c   do 10 i=n+1,nn
      v(8) = 1.0
      v(9) = 0.0
      v(10)= 0.0
      v(11)= 1.0
c10  continue
c   do 20 i=1,n
c   v((n+1)*i)=1.0
c20  continue
c
c print *, v
c
      do 100 m=1,nstep
c
      do 25 j=1,irate
c
c *****
c
      do 26 i=1,nn
        y(i)=v(i)
26  continue
      t=tme
      call fcn(t,y,yprime,nn1,be,idc,iac,omega,cou,q,dd,ll,ee)
      do 27 i=1,nn
        A(i)=yprime(i)
27  continue
c
c *****
```

```
c
      do 28 i=1,nn
         y(i)=v(i)+(stpsze*A(i))/2.0
28      continue
         t=tme+stpsze/2.0
         call fcn(t,y,yprime,nn1,be,idc,iac,omega,cou,q,dd,ll,ee)
         do 29 i=1,nn
            B(i)=yprime(i)
29      continue
c
c *****
c
      do 30 i=1,nn
         y(i)=v(i)+(stpsze*B(i))/2.0
30      continue
         t=tme+stpsze/2.0
         call fcn(t,y,yprime,nn1,be,idc,iac,omega,cou,q,dd,ll,ee)
         do 31 i=1,nn
            C(i)=yprime(i)
31      continue
c
c *****
c
      do 32 i=1,nn
         y(i)=v(i)+(stpsze*C(i))
32      continue
         t=tme+stpsze
         call fcn(t,y,yprime,nn1,be,idc,iac,omega,cou,q,dd,ll,ee)
         do 33 i=1,nn
            D(i)=yprime(i)
33      continue
c
c *****
```

```
c
    do 34 i=1,nn
        v(i)=v(i)+stpsze*(A(i)+D(i)+2.0*(B(i)+C(i)))/6.0
34    continue
        tme=tme+stpsze
c
c *****
c
c      Steps to give time-delay to the system
    do 555 mm=q-1,1,-1
        ll(mm+1)=ll(mm)
555    continue
        ll(1)=v(5)
c
    do 556 o=q-1,1,-1
        dd(o+1)=dd(o)
556    continue
        dd(1)=v(2)
c
    do 557 oo=q-1,1,-1
        ee(oo+1)=ee(oo)
557    continue
        ee(1)=v(7)
c
c      write(3,333) v(5),ll(10),v(2),dd(10),v(7),ee(10)
c333    format(1x,f12.6,2x,e12.6,2x,e12.6,2x,e12.6,2x,e12.6,2x,e12.6,2x,e12.6)
c
25    continue
c
c      construct new orthonormal basis by gram-schmidt orthogonalization
c
c      normalize first vector
znorm(1) = 0.0
```

```

do 38 j = 0,1
    znorm(1)=znorm(1)+v(n+2*j+1)**2
38  continue
    znorm(1) = sqrt(znorm(1))
do 40 j = 0,1
    v(n+2*j+1)=v(n+2*j+1)/znorm(1)
40  continue
c    generate new orthonormal set
c    make j-1 gsr coefficients
c
c    do 80 j=2,n
c    gg = 2
c    j = 2
c
do 50 k=1,j-1
    gsc(k)=0.0
    do 50 l=1,2
        gsc(k)=gsc(k)+v(n+2*l)*v(n+2*l-1)
50  continue
c    construct a new vector
do 60 k=1,2
    do 60 l=1,j-1
        v(n+2*k)=v(n+2*k)-gsc(l)*v(n+2*k-1)
60  continue
c    calculate the vector's norm
c
znorm(j)=0.0
do 70 k=1,2
    znorm(j)=znorm(j)+v(n+2*k)**2
70  continue
znorm(j)=sqrt(znorm(j))
c
c    normalize the new vector

```

```
c
      do 80 k=1,2
          v(n+2*k)=v(n+2*k)/znorm(j)
80    continue
c      update running vector magnitudes
c
      do 90 k=1,2
          cum(k)=cum(k)+log(znorm(k))/log(2.0)
90    continue
c
      if(mod(m,io).ne.0) goto 100
      write(2,334) cou,(cum(k)/tme,k=1,2)
334   format(1x,f12.6,2x,e12.6,2x,e12.6)
c
100   continue
1000  continue
      close(1)
      close(2)
c close(3)
      end
c *****
c
      subroutine fcn(t,y,yprime,nn1,be,idc,iac,omega,cou,q,dd,ll,ee)
c
      implicit none
      integer nn1,i,q
      double precision t,y(nn1),yprime(nn1),be,idc,iac,omega,cou
      double precision dd(q),ll(q),ee(q)
c      Nonlinear coupled Josephson junction
      yprime(1)=y(2)
      yprime(2)=-be*y(2)-sin(y(1))+idc+iac*cos(y(3))-cou*(y(2)-ll(q))
      yprime(3)=omega
      yprime(4)=y(5)
```

```

yprime(5)=-be*y(5)-sin(y(4))+cou*(dd(q)+ee(q)-2*y(5))
yprime(6)=y(7)
yprime(7)=-be*y(7)-sin(y(6))+idc+iac*cos(y(3))-cou*(y(7)-ll(q))
c
c   Linearized Josephson junction
c
do 10 i=0,1
yprime(8+i)=y(10+i)
yprime(10+i)=(-be-cou)*y(10+i)-cos(y(1))*y(8+i)
10 continue
c
return
end

```

A.2 Finite Difference method for a semian- nular Josephson Junction

```

clear all
close all
clc
N      = 1500 ;      Number of Grid points
SSTEP = 0.01 ;      Grid Size in distance
TSTEP = 0.02;       Grid Size in time
ITN    = 27300;     Total number of iterations
STBITN = 26250;     Number of iterations for stabilization
ALPHA  = 0.05 ;     Dissipation parameter
BETA   = 0.02;      Dissipation parameter
IL1    = (N/2)*SSTEP; Initial location
idc    = 0.2 ;      dc-bias
iac    = 0.0 ;      ac-bias
ome    = 0.3 ;      frequency of the ac-bias
VEL1   = 0.0;       Initial velocity of fluxon

```

A.2 Finite Difference method for a semiannular Josephson Junction

123

```

abc      = 1;
a = zeros(1,N) ; b=zeros(1,N) ; c=zeros(1,N);
d = zeros(1,N) ;
cout=zeros(1,N) ; dout=zeros(1,N) ;
buf1=zeros(1,N) ; buf2=zeros(1,N) ; buf3=zeros(1,N);
g=zeros(1,N) ; time=0.0;
% /----- Coefficients -----*/
c1 = BETA + TSTEP;
c2 = -(ALPHA * (SSTEP*SSTEP) + (2.0 * (SSTEP*SSTEP)))/
      TSTEP + 2.0 * BETA + 2.0 * TSTEP);
c3 = BETA - TSTEP;
c4 = (ALPHA * (SSTEP*SSTEP) - (2.0 * (SSTEP*SSTEP)))/
      TSTEP + 2.0 * BETA - 2.0 * TSTEP);
c5 = -( (4.0 * (SSTEP*SSTEP))/TSTEP);
c6 = 2.0 * (SSTEP*SSTEP) * TSTEP;
% /*----- Matrix Elements -----*/
a=[0,c1*ones(1,N-2),2.0*c1];
b=[c2*ones(1,N)];
c=[2.0*c1,c1*ones(1,N-2),0];
%/*----- Initial Fluxon solution -----*/
while(iac<=0.6)
    i=1:N;
    buf1(i) = 4*atan(exp((i*SSTEP-IL1)/ sqrt(1-VEL1*VEL1)));
    buf2(i) = 4*atan(exp((i*SSTEP-IL1- VEL1*TSTEP)/
        sqrt(1-VEL1*VEL1)));
    buf3(i) = 0.0;
        k = STBITN;
        k1 = k;
        ESP = 0.0;
    for j=1:ITN+10
%/*----- Predictor -----*/
d(1) = (2*c3)*buf1(2)-c4 * buf1(1) + c5*buf2(1)
        +c6*(ESP*cos(0.0)+ sin(buf2(1)) + idc + iac*sin(ome*time));

```

```

for i=2:N-1
    d(i) = c3*buf1(i-1) - c4 * buf1(i) + c3*buf1(i+1) + c5*buf2(i)
           +c6*(ESP*cos(3.14*i/N)+ sin(buf2(i)) +idc + iac*sin(ome*time));
end

    d(N) =(2*c3)*buf1(N-1)- c4 * buf1(N) + c5*buf2(N)+
           +c6*( ESP*cos(3.14)+sin(buf2(N)) + idc + iac*sin(ome*time));
cout(1)   = c(1)/b(1);
dout(1)   = d(1)/b(1);

for i=1:N-1
    cout(i+1) = c(i+1) / (b(i+1) - (a(i+1)*cout(i)));
    dout(i+1) = (d(i+1) - (a(i+1)*dout(i)))/
                (b(i+1) - (a(i+1)*cout(i)));
end

buf3(N) = dout(N);

for i=N-1:-1:1
    buf3(i) = dout(i) - cout(i)*buf3(i+1);
end
/*----- Corrector -----*/
d(1) = (2*c3)*buf1(2)-c4 * buf1(1) + c5*buf2(1)
        + c6*(ESP*cos(0.0)+ (sin(buf1(1))+sin(buf3(1)))/2)
        + idc + iac*sin(ome*time));

for i=2:N-1
    d(i) = c3*buf1(i-1) - c4 * buf1(i) + c3*buf1(i+1) + c5*buf2(i)
           + c6*(ESP*cos(3.14*i/N)+ (sin(buf1(i))+sin(buf3(i)))/2)
           +idc + iac*sin(ome*time));
end

```


A.2 Finite Difference method for a semiannular Josephson Junction

125

```
d(N) =(2*c3)*buf1(N-1)- c4 * buf1(N) + c5*buf2(N)
      + c6*( ESP*cos(3.14)+(sin(buf1(N))+sin(buf3(N)))/2)
      + idc + iac*sin(ome*time));
cout(1)  = c(1)/b(1);
dout(1)  = d(1)/b(1);

for i=1:N-1
    cout(i+1) = c(i+1) / (b(i+1) - (a(i+1)*cout(i)));
    dout(i+1) = (d(i+1) - (a(i+1)*dout(i)))/(b(i+1)
        - (a(i+1)*cout(i)));
end
buf3(N) = dout(N);
for i=N-1:-1:1
    buf3(i) = dout(i) - cout(i)*buf3(i+1);
end
%/*----- Final State -----*/
    if( j == STBITN)
        tdev1 = sum(buf3);
    end
    if( j == ITN)
        tdi = sum(buf3);
    end
%/*-----*/
if(j>=k1)
    t=1:N-2;
    phi1(t) = (buf3(t+2) - buf3(t))/(2*SSTEP);

    t=1:N;
    phi2(t) = (buf1(t) - buf3(t))/(2*TSTEP);
    k1 = k1 + 30;
end
% /*----- Swapping buffers -----*/
for i=1:N
```

```
        buf1(i) = buf2(i);
        buf2(i) = buf3(i);
    end
time=time+TSTEP;
end
/*-----j loop ----- Iteration loop ends
    ftdev1 = (tdev1 - td1)/N;
    tdev3   = ftdev1/((ITN-STBITN)*TSTEP);
    iacn(abc)=iac;
    voltage(abc) = tdev3;
    velocity(abc) = tdev3*(N*SSTEP/6.283);
    abc=abc+1;
    iac=iac+0.0001;
end
plot(buf3)
figure; plot(voltage,iacn,'k.','markersize',10)
figure; plot(velocity,iacn,'k.','markersize',10)
% /***** -- THE END -- *****/
```

Bibliography

- [1] Kristian Fosshem and Asle Sudbø, *Superconductivity: Physics and Applications*, John Wiley & Sons (2004).
- [2] B D Josephson, *Phys. Lett. A* **7**, 251 (1962).
- [3] J R Anderson and J M Rowell, *Phys. Rev. Lett.* **10**, 230 (1963).
- [4] J. R. Waldram, *Rep. Prog. Phys.* **39**, 751 (1976).
- [5] A. Barone and G. Paterno, *Physics and Applications of Josephson effect*, Wiley & sons, New York (1982).
- [6] K K Likharev, *Dynamics of Josephson junctions and circuits*, Gordon and Breach Science Publishers (1982).
- [7] W. C. Stewart, *Appl. Phys. Lett.* **12**, 277 (1968).
- [8] Mc Cumber, *J. Appl. Phys.* **39**, 3113 (1968).
- [9] A. Wallraff, *PhD Thesis*, (2000).
- [10] N. Thyssen, *PhD Thesis*, (1999).
- [11] A. Kemp, *Diploma Thesis*, (2001).

-
- [12] P.D. Shaju and V.C. Kuriakose, Phys. Rev. B **65**, 214508 (2002).
- [13] P.D. Shaju and V.C. Kuriakose, Physica C **383**, 395 (2003) .
- [14] P.D. Shaju and V.C. Kuriakose, Physica C **434**, 25 (2006).
- [15] M. Lakshmanan and S. Rajasekar, *Nonlinear Dynamics: Integrability, Chaos and Patterns*, Springer-Verlag Heidelberg (2005).
- [16] S.L. Ross, *Differential Equations*, John Wiley & Sons, Third Edition (1984).
- [17] D. V. Anosov, Proc. Steklov Inst. Math **90**, 1 (1967).
- [18] R. Bowen, Amer. J. Math **92**, 725 (1970).
- [19] S. M. Hammel, J. A. Yorke and C. Grebogi, J. Complexity **3**, 136 (1987).
- [20] S. H. Strogatz, *Nonlinear Dynamics and Chaos*, Perseus Books (1994).
- [21] E. Ott, *Chaos in Dynamical Systems*, Cambridge University Press (1993).
- [22] E. N. Lorentz, J. Atmos. Sci. **20**, 33 (1964).
- [23] Alan Wolf, Jack B. Swift, Harry L. Swinney, John A. Vastano, Physica D **16**, 285 (1985).
- [24] E. Hopf, Commun. Pure. Appl. Math **1**, 303 (1948).

-
- [25] D. Ruelle and F. Takens, *Commun. Pure. Appl. Math* **20**, 167 (1971).
- [26] R.L.Kautz, *IEEE Trans. Magn.* **19**, 465 (1983).
- [27] P. Holmes, *Phys. Rep.* **193**, 137 (1990).
- [28] V. N. Belykh, N. F. Pedersen and O. H. Christiansen, *Phys. Rev. B* **16**, 4860 (1977).
- [29] B. A. Huberman, J. P. Crutchfield and N. H. Packard, *Appl. Phys. Lett.* **37**, 750 (1980).
- [30] K. Fesser, A. R. Bishop and P. Kumar, *Appl. Phys. Lett.* **43**, 123 (1983).
- [31] W. C. Schieve, A. R. Bulsara and E. W. Jacobs, *Phys. Rev. E* **37**, 3541 (1988).
- [32] Ezequiel N. Pozzo and Daniel Domínguez, *Phys. Rev. Lett.* **98**, 057006 (2007).
- [33] H. Schulze, R. Behr, F. Möller, and J. Niemeyer, *Appl. Phys. Lett.* **73**, 996 (1998).
- [34] P. Benz and C. A. Hamilton, *Appl. Phys. Lett.* **68**, 3171 (1996).
- [35] R.L. Kautz and R. Monaco, *J.Appl.Phys.* **57**, 875 (1985).
- [36] D.F. D’Humieres, M. R. Beasley, B. A. Huberman, and A. Libchaber, *Phys. Rev. E* **26**, 3483 (1982).
- [37] Y. Braiman and I. Goldhirsch, *Phys. Rev. Lett.* **66**, 2545 (1991).

- [38] W. H. Steeb and A. Kunick, *Phys. Rev. A.* **25**, 2889 (1982).
- [39] R. L. Kautz, *Rep. Prog. Phys.* **59**, 935 (1996).
- [40] T. Kapitaniak, *Controlling Chaos*, Academic press, San Diego, 1996.
- [41] T. Kapitaniak and S. R. Bishop, *The illustrated dictionary of nonlinear dynamics and chaos*, John Wiley and sons, Newyork, 1999.
- [42] A. Pikovsky, M. Rosenblum and J. Kurths, *Synchronization: A Universal concept in Nonlinear Science*, Cambridge University press, Cambridge, 2001.
- [43] T. Yamada and H. Fujisaka, *Prog. Theor. Phys.* **69**, 32 (1983).
- [44] T. Yamada and H. Fujisaka, *Prog. Theor. Phys.* **70**, 1240 (1983).
- [45] C.-M. Kim, S. Rim, and W.-H. Kye, *Phys. Rev. Lett.* **88**, 014103 (2002).
- [46] L. M. Pecora and T. L. Carroll, *Phys. Rev. Lett.* **64**, 821 (1990).
- [47] S. Boccaletti, J. Kurths, G. Osipov, D.L. Valladares and A. S. Pikovsky, and C.S. Zhou, *Phys. Rep.* **366**, 1 (2002).
- [48] M. G. Rosenblum, A. S. Pikovsky, and J. Kurths, *Phys. Rev. Lett.* **76**, 1804 (1996).
- [49] Reggie Brown and Ljupco Kocarev, *Chaos* **10**, 344 (2000).
- [50] K Pyragas, *Phys. Rev. E* **54**, R4508 (1996).

-
- [51] L. M. Pecora and T. L. Carroll, Phys. Rev. A. **44**, 2374 (1991).
- [52] R. He and P. G. Vaidya, Phys. Rev. A. **46**, 7387 (1992).
- [53] T. Kapitaniak, Phys. Rev. E. **50**, 1642 (1994).
- [54] M.A. Zaks, E.-H Park, M. G. Rosenblum and J. Kurths, Phys. Rev. Lett. **82**, 4228 (1999).
- [55] N. F. Rulkov, M. M. Sushchik, L.S. Tsimring and H. D. I Abarbanel, Phys. Rev. E. **51**, 980 (1995).
- [56] L. Kocarev and U. Parlitz Phys. Rev. Lett. **74**, 5028 (1995).
- [57] L. M. Pecora, T. L. Carroll, G. A. Johnson, D. J. Mar and J. F. Heagy , Chaos **7**, 520 (1997).
- [58] N. Grønbech-Jensen, P.S.Lomdahl and M.R.Samuelsen, Phys. Rev. B **43**, 12799 (1991).
- [59] D.C.Cronemeyer, C.C.Chi,A.Davidson and N.F.Pedersen, Phys. Rev. B **31**, 2667 (1985).
- [60] Wenhua Hai, Yi Xiao, Guishu Chong, Qiongtao Xie Phys. Lett. A **295**, 220 (2002).
- [61] W.J.Yeh, O.G.Symko and D.J.Zheng, Phys. Rev. B **42**, 4080 (1990).
- [62] R.L.Kautz and J.C.Macfarlane, Phys. Rev. A **33**, 498 (1986).
- [63] E. Abraham, I. L. Atkin and A. Wilson, IEEE Trans.Appl. Supercond. **9**, 4166 (1999) .

- [64] A. N. Grib, P. Seidel, and J. Scherbel *Phys. Rev. B* **65**, 094508 (2002).
- [65] A. Uçar, K. E. Lonngren and Er-Wei Bai, *Chaos Soliton and Fractals* **31**, 105 (2007).
- [66] P. Barbara, A. B. Cawthorne, S. V. Shitov and C.J.Lobb , *Phys. Rev. Lett.* **82**, 1963 (1999).
- [67] B. Vasilie, S. V. Shitov, C.J.Lobb and P. Barbara, *Appl. Phys. Lett.* **78**, 1137 (2001).
- [68] W. A. Al-Saidi and D. Stroud, *Phys. Rev. B* **65**, 224512 (2002).
- [69] G. Filatrella, N. F. Pedersen and K. Wiesenfeld, *Phys. Rev. E* **61**, 2513 (2000).
- [70] A. E. Koshelev and L. N. Bulaevskii, *Phys.Rev.B* **77**, 014530 (2008).
- [71] J.A.Blackburn, G.L.Baker and H.J.T.Smith, *Phys. Rev. B* **62**, 5931 (2000).
- [72] A. A. Cherinkov and G. Schmidt, *Phys. Rev. E* **52**, 3415 (1995).
- [73] A. B. Cawthorne, P. Barbara, S. V. Shitov, C.J.Lobb and K. Wiesenfeld , *Phys. Rev. B* **60**, 7575 (1999).
- [74] D Dominguez and H. A. Cerdcira, *Phys. Rev. Lett.* **71**, 3359 (1993).
- [75] I. Shimada and T. Nagashima, *Prog. Theor. Phys.* **61**, 1605 (1979).

-
- [76] G. Benettin, L. Galgani, A. Giorgilli and J. -M. Strelcyn, *Mec-*
canica **15**, 9 (1980).
- [77] E. Ott, C. Grebogi and J. A. Yorke, *Phys. Rev. Lett.* **64**, 1196
(1990).
- [78] J.Singer, Y.-Z.Wang and Haim.H.Bau, *Phys. Rev. Lett.* **66**,
1123 (1991).
- [79] A. G. Balanov, N. B. Janson, and E. Schöll, *Phys. Rev. E* **71**,
016222 (2005).
- [80] K. Pyragus, *Phys. Lett. A* **170**, 421 (1992).
- [81] R. Lima and M. Pettini, *Phys. Rev. A* **41**, 726 (1990).
- [82] F. Cuadros and R. Chacon, *Phys. Rev. E* **47**, 4628 (1993).
- [83] Y. S. Kivshar, F. Rodelsperger and H. Benner, *Phys. Rev. E*
49, 319 (1994).
- [84] Y. Liu and J. R. Leite, *Phys. Lett. A* **185**, 35 (1994).
- [85] M. Salerno, *Phys. Rev. B* **44**, 2720 (1991).
- [86] L. Fronzoni, M. Giocodo and M. Pettini, *Phys. Rev. A* **43**, 6483
(1991).
- [87] A. Azevedo and S. M. Rezende, *Phys. Rev. Lett.* **66**, 1342
(1991).
- [88] W. X. Ding, H. Q. Shc, W. Huang and C. X. Yu *Phys. Rev.*
Lett. **72**, 96 (1994).

-
- [89] C. Y. Soong, W. T. Huang, F. P. Lin, and P. Y. Tzeng, Phys. Rev. E **70**, 016211 (2004).
- [90] Chol-Ung Choe, Klaus Höhne, Hartmut Benner, and Yuri S. Kivshar, Phys. Rev. E **72**, 036206 (2005).
- [91] W. -H. Steeb, J. A. Louw and T. Kapitaniak, J. Phys. Soc. Japn **55**, 3279 (1986).
- [92] T. Kapitaniak, J. Awrejcewicz and W. -H. Steeb, J. Phys. A, **20**, L355 (1987).
- [93] T. Kapitaniak, *Chaos in systems with noise*, World Scientific, Singapore, 1988.
- [94] Zhilin Qu, Gang Hu, Guojain Yang and Guangrong Qin, Phys. Rev. Lett. **74**, 1736 (1995).
- [95] H.W.Yin, J.H.Dai and H.J. Zhang, Phys. Rev. E **58**, 5683 (1998).
- [96] F. X. Hebrank, E. Vollmer, P. Gutmann, F. Müller and J. Niemeyer, *Nonlinear Superconducting Devices and High T_c Materials*, World Scientific, Singapore, p.461 (1995).
- [97] K. K. Likharev and V. K. Semenov, IEEE Trans. Appl. Supercond. **1**, 3 (1991).
- [98] K. Nakajima, H. Mizusawa, H. Sugahara and Y. Sawada, IEEE Trans. Appl. Supercond. **1**, 29 (1991).
- [99] Y. Mizugaki, K. Nakajima, Y. Sawada and T. Yamashita, Appl. Phys. Lett. **62**, 762 (1993).

-
- [100] A. M. Kadin *J. Appl. Phys.* **68**, 5741 (1990).
- [101] M. T. Levinsen, R. Y. Chiao, M. J. Feldman and B. A. Tucker, *Appl. Phys. Lett.* **31**, 776 (1977).
- [102] J. R. Terry et.al, *Phys. Rev. E* **59**, 4036 (1999).
- [103] J. W. Shuai and K. W. Wong, *Phys. Rev. E* **57**, 7002 (1998).
- [104] V. M. Eguíluz, D. R. Chialvo, G. A. Cecchi, M. Baliki, and A. V. Apkarian, *Phys. Rev. Lett.* **94**, 018102 (2005).
- [105] I. Fischer, R. Vicente, J. M. Buldú, M. Peil, C. R. Mirasso, M. C. Torrent and J. Garcöa-Ojalvo, *Phys. Rev. Lett.* **97**, 123902 (2006).
- [106] M. S. Baptista, C. Zhou, and J. Kurths, *Chinese Phys. Lett.* **23**, 560 (2006).
- [107] J. Hale, *Functional Differential Equations*, Springer-Verlag, New York, 1971.
- [108] L. M. Pecora and T. L. Carroll, *Phys. Rev. Lett.* **80**, 2109 (1998).
- [109] U.E. Vincent et.al, *Chaos* **14**, 1018 (2004).
- [110] A. S. Landsman and I. B. Schwartz, *Phys. Rev. E* **75**, 026201 (2007).
- [111] M. G. Rosenblum, A. S. Pikovsky, and J. Kurths, *Phys. Rev. Lett.* **78**, 4193 (1997).

- [112] J. D. Farmer, *Physica D* **4**, 366 (1982).
- [113] J. K. White, M. Matus and J. V. Moloney, *Phys. Rev. E* **65** , 036229 (2002).
- [114] T. Heil, I. Fischer, W. Elsasser, J. Mulet and C. R. Mirasso, *Phys. Rev. Lett.* **86** , 795 (2001).
- [115] J. Mulet, C. R. Mirasso, T. Heil and I. Fischer *J. Optics B* **6** , 97 (2004).
- [116] L. B. Shaw, I. B. Schwartz, E. A. Rogers and R. Roy, *Chaos* **16** , 015111 (2006).
- [117] Feng Cun-Fang, Zhang Yan and Wang Ying-Lai, *Chin. Phys. Lett.* **23**, 1418 (2006).
- [118] Feng Cun-Fang, Zhang Yan and Wang Ying-Lai, *Chin. Phys. Lett.* **24**, 50 (2007).
- [119] D. V. Senthilkumar, M. Lakshmanan, and J. Kurths, *Phys. Rev. E* **74**, 035205 (2006).
- [120] C. Masoller, *Phys. Rev. Lett* **86**, 2782 (2001).
- [121] S. Sivaprakasam, E. M. Shahverdiev, P. S. Spencer and K. A. Shore, *Phys. Rev. Lett* **87**, 154101 (2001).
- [122] N.Krasovskii, *Stability of motion*, Stanford press, Stanford, 1963.
- [123] K.Pyragas, *Phys. Rev. E* **58**, 3067 (1998).

-
- [124] D. V. Senthilkumar and M. Lakshmanan, *Chaos* **17**, 013112 (2007).
- [125] Ira B. Schwartz and Leah B Shaw, *Phys. Rev. E* **75**, 046207 (2007).
- [126] V. K. Kaplunenko, M. I. Khablpov and E. B. Goldobin, *Supercond. Sci Technol.***4**, 674 (1991).
- [127] G. V. Osipov, A. S. Pikovsky, and J. Kurths, *Phys. Rev. Lett.* **88**, 054102 (2002).
- [128] Chitra R Nayak and V.C. Kuriakose, *Phys.Lett.A* **365**, 284 (2007).
- [129] F. Nguyen et.al, *Phys.Rev.Lett.* **99**, 187005 (2007).
- [130] T. Nagatsuma, K. Enpuku, F. Irie and K.Yoshida, *J. Appl. Phys.* **63**, 1130 (1983).
- [131] M. Jaworski, *Supercond. Sci. Technol.* **21**, 065016 (2008).
- [132] Y. Nakamura, Y.A. pashkin, and J.S. Tsai, *Nature* **398**, 786 (1999).
- [133] P.D. Shaju and V.C. Kuriakose, *Phys.Lett. A* **267**, 420 (2000).
- [134] H Tanaka, Y Sekine, S Saito and H Takayanagi, *Supercond. Sci. Technol.* **14**, 1161 (2001).
- [135] Y. Makhlin, G. Schon, and A. Shnirman, *Rev.Mod.Phys.***73**, 357 (2001).

- [136] I.V. Vernik et.al, J.Appl.Phys. **81**, 1335 (1997).
- [137] S. Kiel et.al. Phys.Rev. B **54**, 14948 (1996).
- [138] D.W. McLaughlin and A.C. Scott, Phys.Rev. A **18**, 1652 (1978).
- [139] P.S. Lomdahl, O.H. Sorensen, and P.L. Christiansen, Phys.Rev. B **25**, 5737 (1982).
- [140] A.V. Ustinov et.al, Phys.Rev.Lett. **69**, 1815 (1992).
- [141] P.D. Shaju and V.C. Kuriakose, Phys.Rev.B **70**, 064512 (2004).
- [142] P.D. Shaju and V.C. Kuriakose, Supercond. Sci. Technol. **16**, L25 (2003).
- [143] P.D. Shaju and V.C. Kuriakose, Phys.Lett. A **299**, (2002) 628, Pis'ma v ZhETF, **76**, 14 (2002).
- [144] E. Goldobin, B. A. Malomed and A. V. Ustinov, Phys.Rev.E **65**, 056613 (2002).
- [145] Niels Grønbech-Jensen and M. Cirillo, Phys.Rev.B **70**, 214507 (2004).
- [146] L. Morales-Molina, F. G. Mertens and A. Sánchez, Phys.Rev.E **73**, 046605 (2006).
- [147] N. Grønbech-Jensen, P.S.Lomdahl and M.R.Samuelsen, Phys. Lett. A **154**, 14 (1991).

Tu05

BIBLIOGRAPHY

139

- [148] A. L. Pankratov, A. S. Sobolev, V. P. Koshelets and J. Mygind, Phys.Rev.B **75**, 184516 (2007).
- [149] L. E. Guerrero and M. Octavio, Phys.Rev.A **40**, 3371 (1999).
- [150] J. Rubinstein, J. Math. Phys. **11**, 258 (1970).
- [151] P.L.DeVries, *A First Course in Computational Physics*, John Wiley & Sons, NewYork, (1994).
- [152] S. Sakai and M. R. Samuelsen, Appl. Phys. Lett. **50**, 1107 (1987).
- [153] O. H. Olsen and M. R. Samuelsen, Phys. Lett. A **266**, 123 (2000).

